DIPARTIMENTO DI IDRAULICA, TRASPORTI ED INFRASTRUTTURE CIVILI
POLITECNICO DI TORINO

Chiara Barberis[1], Peter Molnar[2],
Pierluigi Claps[1], Paolo Burlando[2]

(1) Politecnico di Torino [*chiara.barberis@polito.it*] [*claps@polito.it*]

(2) ETH Zurich [*molnar@ihw.ethz.ch*] [*burlando@ihw.ethz.ch*]

HYDROLOGIC SIMILARITY OF RIVER BASINS THROUGH REGIME STABILITY

Working Paper 2003 - 03
Ottobre 2003

Abstract

The seasonality of streamflow can vary widely from river to river and is influenced mostly by the local seasonal cycles of precipitation and evaporation demand, by the timing of snowmelt (if any), as well as by travel times of the groundwater component of runoff. Traditionally, streamflow regimes have been analyzed from a static point of view to produce classifications useful to a prior general understanding of the similarità and differences of different rivers across wide regions. Methods for systematic clas-sification have been proposed in the recent years but rarely quantitative values have been provided to characterise numerically specific features of the seasonal evolution of streamflows.

The aim is twofold: (1) to select some quantitative indices able to objectively distinguish slightly or greatly different average seasonal streamflow pat-terns, and (2) to use some of the above indices to detect possible changes in the seasonality of streamflows over the last 30 years, which may be the result of a natural or anthropogenic non-stationarity. Indices used to investigate task (1) are essentially obtained through Fourier analysis, moments and the Informational Entropy Concept. Similar indices have been adapted to the 12-months runoff sequence over the data record length and used to investigate task (2). The analysis has been carried out on 53 basins in Switzerland, on data records related to the period 1971-2000, showing that the envisaged seasonal indices have a good capability of discrimination of rivers with different climatic and physiographic characteristics, which makes the work in-teresting for validation of hydrological mapping studies. Although in the examined records trend analysis does not show large temporal anomalies (i.e. seasonal shifts) of streamflow regimes, the analysis framework offers an additional and non-conventional objective methodology to detect non-stationarity and the related anomalies.

1. Introduction

1.1 Motivation and Framework.

It has been widely assessed that the atmospheric concentration of some of the greenhouse gases like carbon dioxide, nitrous oxygen, methane and clorofluorocarbons has increased in the last decades as a consequence of human activities. This is expected to lead to significant changes in regional and global climate patterns, as a consequences of the re-emission of long-wave radiation back to the Earth.

A number of methodologies have been identified and proposed by the scientific community to analyze the consequences of the greenhouse effect. Accordingly, the

physically based three dimensional mathematical modelling of the atmospheric circulation through GCMs (Global Circulation Model) represents the most flexible and promising route to systematic studies concerned with climate change and its impacts on natural processes. Unfortunately, GCMs provide climate and hydrologic variables prediction at a large scale, according to a space defined by the grid used for model integration that is typically not finer that 2.5°x3.5° in longitude and latitude. GCMs cannot therefore accurately represent hydrological processes at proper regional scales, as these are integrated over a coarse space grid, which is much larger than the characteristic space variability of the processes. The output of the GCMs must then be disaggregated to a local scale in order to investigate the impact of climate change on water resources at scales required by water engineering.

The underlying approach of this work is to allow hydrological data to speak for themselves. Deductive models, so dominant in hydrological analyses, have been given a low priority in favour of inductive methods based on statistical theory.

1.2 Climate and Weather.

Weather and climate have a profound influence on life on Earth. They are part of the daily experience of human beings and are essential for health, food production and well-being.

Many consider the prospect of human-induced climate change as a matter of concern. In common parlance the notions “weather” and “climate” are loosely defined.

The “weather”, as we experience it, is the fluctuating state of the atmosphere around us, characterised by the temperature, wind, precipitation, clouds and other weather elements. This weather is the result of rapidly developing and decaying weather systems such as mid-latitude low and high pressure systems with their associated frontal zones, showers and tropical cyclones. Weather has only limited predictability.

Mesoscale convective systems are predictable over a period of hours only; synoptic scale cyclones may be predictable over a period of several days to a week. Beyond a week or two individual weather systems are unpredictable. “Climate” refers to the average weather in terms of the mean and its variability over a certain time-span and a certain area.

Classical climatology provides a classification and description of the various climate regimes found on Earth. Climate varies from place to place, depending on latitude, distance to the sea, vegetation, presence or absence of mountains or other geographical factors.

Climate varies also in time; from season to season, year to year, decade to decade or on much longer time-scales, such as the Ice Ages. Statistically significant variations of the mean state of the climate or of its variability, typically persisting for decades or longer, are referred to as “climate change”.

Climate variations and change, caused by external forcing, may be partly predictable, particularly on the larger, continental and global, spatial scales. Because human activities, such as the emission of greenhouse gases or land-use change, do result in external forcing, it is believed that the large-scale aspects of human-induced climate change are also partly predictable. However the ability to actually do so is limited because we cannot accurately predict population change, economic change, technological development, and other relevant characteristics of future human activity.
In practice, therefore, one has to rely on carefully constructed scenarios of human behaviour and determine climate projections on the basis of such scenarios.

1.3 Climatic variables

The traditional knowledge of weather and climate focuses on those variables that affect daily life most directly: average, maximum and minimum temperature, wind near the surface of the Earth, precipitation in its various forms, humidity, cloud type and amount, and solar radiation. These are the variables observed hourly by a large number of weather stations around the globe. However this is only part of the reality that determines weather and climate. The growth, movement and decay of weather systems depend also on the vertical structure of the atmosphere, the influence of the underlying land and sea and many other factors not directly experienced by human beings.

Climate is determined by the atmospheric circulation and by its interactions with the large-scale ocean currents and the land with its features such as albedo, vegetation and soil moisture.

The climate of the Earth as a whole depends on factors that influence the radiative balance, such as for example, the atmospheric composition, solar radiation or volcanic eruptions. To understand the climate of our planet Earth and its variations and to predict the changes of the climate brought about by human activities, one cannot ignore any of these many factors and components that determine the climate.

We must understand the climate system, the complicated system consisting of various components, including the dynamics and composition of the atmosphere, the ocean, the ice and snow cover, the land surface and its features, the many mutual

interactions between them, and the large variety of physical, chemical and biological processes taking place in and among these components.

"Climate" in a wider sense refers to the state of the climate system as a whole, including a statistical description of its variations. This chapter provides the reader with an overview of the climate system and the climate in this wider sense.

1.4 The Greenhouse Effect.

The climate of the Earth is always changing. In the past it has altered as a result of natural causes. Nowadays, however, the term climate change is generally used when referring to changes in our climate which have been identified since the early part of the 1900's.

The changes we have seen over recent years and those which are predicted over the next eighty years are thought to be mainly as a result of human behaviour rather than due to natural changes in the atmosphere.

The greenhouse effect is very important when we talk about climate change as it relates to the gases which keep the Earth warm.

It is the extra greenhouse gases which humans have released which are thought to pose the strongest threat.

2. River Regimes Classification

2.1 Seasonality and River Flow Regime.

The seasonality of streamflow can vary widely from river to river and is influenced mostly by the local seasonal cycle of precipitation, the local seasonal cycle of evaporation demand, the timing of snowmelt (if any), as well as by travel times of the groundwater component of runoff. Antropic alterations must also be carefully checked and, if it is possible, filtered out to obtain the natural seasonal cycle.

In general, not just the timing but the amount of streamflow can depend on, and directly reflect, precipitation timing.

However, basin characteristics, human influences and snow accumulation and melting can have a notable influence on the precipitation – runoff seasonal relations. By the spatial variability viewpoint there can be many exceptions to the large scale patterns of streamflow seasonality than are found, for example, in spatial patterns of precipitation seasonality.

As more and more studies have made progress toward integration and prediction of streamflow conditions on regional and larger scales, often by relating streamflow to global climatic processes and precursors, the need for a large-scale depiction of the pattern of seasonality and inter annual variability of streamflow from all of the earth's land surface has become more pressing.

Seasonality is usually investigated using long records of mean monthly runoff, that allow one to look at the high and low flow seasons within the year, their inter-annual variation and within-season features.In some cases, average daily flows can be analyzed to include additional patterns useful to the knowledge of the monthly runoff composition.

2.2 State of the art in seasonality and regime classification.

Traditionally, world waters have been analyzed from a static point of view to produce maps of water balance elements. Such maps usually show annual values, while seasonal variations are specified in term of classification of climate and river flow regimes.

A variety of flow regime classifications exists, some covering the whole world, other adapted locally. The two most well-known and widely used are those by Lvovich (1938) and Pardé (1955). The flow regime classification suggested by Lvovich is a development of an old (probably the first) genetic global flow regime classification, presented by A.I. Voeikov in 1884. Voeikov differentiated streamflow records between nine types of flow regime, based primarily on climatic features. Two aspects form the basis in Lvovich's classification: genetic source and seasonal distribution of flow. Four genetic sources are identified: snow, rain, glaciers and groundwater. 12 gradations for the four sources and the four seasons, respectively, makes a total of 144 combinations of flow regimes. In reality only 38 proved to exist and they were further grouped into 12 main types for the whole world.

Pardè flow regime classification is global and is based on the genetic sources of flow formation and precipitation distribution within the year. This classification uses the Koppen (1936) climate classification as a starting point, in which three main flow regimes are distinguished: megathermal, mesothermal and microthermal. These are subdivided by Pardè into a number of subgroups in dependence of the distribution of high/low flow.

Both Lvovich's and Pardè's classifications are rather general and the limits used for classification in both of them are quite arbitrary. A suitable flow regime classification should instead be a quantitative one, possibly based on the time distribution of the "genetic" sources of flow within a year.

River flow regimes have been used as diagnostic tools for the output of climate models and in flow sensitivity studies (Krasovskaia 1997). This was made by grouping flow series into regimes type, based on a hierarchical aggregation of monthly flow series into flow regime type. The discriminating criterion used by Krasovskaia is related to the minimization of an entropy-based function. Based on this principle, extensive classification of streamflow regimes were realized by Krasovskaia and Gottschalk.(1992-1993-1994)

As regards recent contribution on the evolution of climatic variables, in terms of the seasonal regime, Vega et al. (1998) described inter-decadal climate variations across the USA, while others have examined variations in temperature and precipitation in different regions of the world over the last few decades. Whitfield and Cannon (2000), analyzed the changes in streamflow and climate records in coastal British Columbia, identifying consistent changes in the hydrologic regime, with six distinctive patterns of hydrologic change. The spatial distribution of these patterns have led them to conclude that, in different ecozones, small variations in temperature generate different hydrologic response. Moreover, by using a statistical clustering procedure, group patterns of seasonal variations in temperature, precipitation and streamflow have been identified across Canada.

One aspect of these recent studies is the finding that small, statistically insignificant, climate variations accompanied statistically sensible changes in the timing of seasonal streamflow patterns.

The river flow regime, describing the average seasonal pattern of flow, reflects climatic and physiographic conditions in a basin. This average pattern can be stable, demonstrating the same seasonality in river flow from year to year, or unstable, when the flow regime alternates between a number of different patterns.

Since year to year variations in streamflow play an important role in development and management of water resources in most regions, we will consider the regime stability as an additional property of the streamflow series.

2.3 Seasonality: a new approach.

The current study aims to devise and apply new indices of streamflow seasonality on streamflow data, in order to examine year to year variations.

The seasonality and year-to-year variations of streamflows can be catalogued to understand linkages between basins and regions, and across time.

Therefore, in regions with no discharge measurements, when estimating flow characteristics, the hydrologist could rely on the discharge regime which best fits basins pysiographic characteristics.

3. Indices of Runoff Regime Stability.

3.1 Regime Analysis.

In the past, analyses in this field have in the past focused on changes in the extremes or total volumes or rainfall and runoff. Only recently, changes in the distributions of daily precipitation and streamflow have been analyzed. (See Zhang *et al.*, 2001; Burn and Hag Elnur, 2002).

In the European Alpine region, recent detailed studies have focused on precipitation trends (Widmann and Schär, 1997; Frei and Schär, 2001), but a thorough analysis of changes in streamflow is lacking.

The area in wich we have focus on regime stability is Switzerland

In the floowing traditional and less common variables, related to the whitin year distribution of runoff are presented.Computation of these variables in the case study is presented in section 3, A iscusion of results and of connections with the basin physiografic parametres closes the paper.

3.2 Variable and Parameters related to seasonality.

The hydrometric variables considered in devising stability indices are:

1. Mean annual streamflow [m^3/s]
2. Mean monthly streamflow [m^3/s]
3. Minimum and maximum annual daily streamflow for each year[m^3/s]
4. Time span underlying half of the runoff volume in each year
5. Parametrers of the Fourier series fitting the streamflow regime in each year
6. Parameters of the Fourier series fitting the average runoff regime
7. Julian day of maximum daily streamflow
8. Julian day of minimum daily streamflow
9. Informational Entropy as a measure of stability of the annual pattern
10. Informational Entropy of the average streamflow regime
11. Pardè coefficient of seasonality

The following basic statistics have also been computed:

1. Mean and variance of daily streamflow.
2. Autocorrelation coefficient of Annual Streamflow.

3. Median of daily streamflow in each year

3.2.1 Mean and Variance.

The mean and the variance of a time series y_t are estimated by:

$$\bar{y} = \left(\frac{1}{N}\right)\sum_{t=1}^{N} y_t$$

$$s^2 = \left(\frac{1}{N-1}\right)\sum_{t=1}^{N} \left(y_t - \bar{y}\right)^2$$

respectively, where N =sample size.

3.2.2 Autocorrelation coefficient.

The autocorrelation coefficient of daily streamflow related to a lag k is estimated by:

$$r_k = \frac{c_k}{c_0}$$

where:

$$c_k = \left(\frac{1}{N}\right)\sum_{t=1}^{N-k} \left(y_{t+k} - \bar{y}\right)\left(y_t - \bar{y}\right)$$

The above coefficient is an estimator of the population autocorrelation coefficient r_k. The plot of $\mathbf{r_k}$ versus k is the correlogram.

The lag-one serial correlation coefficient $\mathbf{r_1}$ is a simple measure of the degree of time dependence of a series.

3.2.3 Time span underlying half of the runoff volume in each year

Time span is investigated to explore the significance of a possible shift in the hydrologic regime.

Time span is defined as the date by which half of the annual total runoff has occurred. A negative trend in the median indicates a shift in the annual streamflow distribution toward an earlier date.

3.2.4 Pardè Coefficients

A number of indices have been considered to characterize the average streamflow regime. The flow regime of a river can be described in terms of the dimensionless Pardè coefficients (PK_i), defined as:

$$PK_i = \frac{\overline{Q_i}}{\overline{Q}}, \quad i = 1,2,\ldots\ldots 12$$

where:

- $\overline{Q_i}$ is the average streamflow in the month i
- $\overline{Q}$ is the average annual streamflow

3.2.5 Informational Entropy : a measure of stability.

The stability of a certain flow regime may be quantitatively expressed by the sum of the entropies related to the occurrence of the regime characteristics (maximum and minimum) in the discriminating periods.

Let us consider a set of *n* events $E_1,\ldots, E_n$ which form a complete system in the sense that it is certain that one of these must occur. Thus, if their probabilities are $p_1,\ldots, p_n$ they should sum up to one:

$$\sum^{n} p_i = 1 \qquad p_i \geq 0, i = 1,\ldots..,n$$

A measure of the uncertainty of an experiment, called entropy of the experiment **H,** can be applied to characterize the uncertainty of the occurrence of a maximum or minimum value within a discriminating period.

Unlike previous approaches, this definition allows us to operate on monthly values of individual years and not only on long-term monthly means. This approaches is an extension of the aggregation theory based on Information Inaccuracy, developed by Theil. Here entropy will be used for optimal grouping of individual monthly flow series into regime types with respect to quantitative discriminating criteria for each regime type.

The stability of maxima or minima of a particular river flow regime is thus characterized by means of the entropy of experiment (Shannon &Weaver, 1941):

$$H = -\sum_{i=1}^{n} p_i \ln(p_i)$$

This expression implies that entropy is a continuous non negative function of the probabilities $p_1, \ldots, p_n$. Entropy is equal to zero only if one of these probabilities equals 1 and all the rest are zero (as $p \to 0, \lim\, p\ln(p) = 0$)

To calculate entropy, for every year we select the month in which the monthly maximum/minimum has occurred. The analysis period is then divided in sub-periods of N years. For the period of observation (N years) the probability that the maximum/minimum falls in a certain month is computed as:

$Pmax_j$ or $Pmin_j = \frac{1}{N} s_j$ $\quad$ j=1,2….12

where s_j is the sum of the occurrences of the maximum/minimum streamflow in the month j.

The stability of maximum and minimum flow regime is then characterized by means of the informational entropy:

$$H_{\max} = -\sum_{j=1}^{12} p_{\max j} \ln(p_{\max j}) \qquad H_{\min} = -\sum_{j=1}^{12} p_{\min j} \ln(p_{\min j})$$

Entropy H reaches its maximum when all the possible values of the events E1, …, En are equally probable: $p_1 = \ldots = p_n = \frac{1}{n}$

In this case the condition $H=\ln(n)$ holds (Maximum entropy). Naturally, the higher the entropy value of an experiment, the smaller is the frequency of observation of a given flow pattern year after year. Thus, entropy may be employ as an 'instability index' of the flow regime type, expressed in terms of the month in which maxima and minima occur.

In a subsequent approach, the concept of entropy is applied to the average regime described by Pardè coefficients, to obtain a number that gives a quantitative measure of uniformity of a river regime. In fact, the ratio between the average monthly streamflow and average annual streamflow (Pardè coefficient) can be seen like a probability p_i:

$$p_i = \frac{PK_i}{\sum_{i=1}^{12} PK_i}$$

Applying the definition of entropy: $H = -\sum_{i=1}^{n} p_i \ln(p_i)$ we obtain an indicator to define a new regime classification in a very simple way.

3.2.6 Fourier Series analysis.

Any continuous function $f(x)$ can be expressed as an infinite sum of (periodic) sine and cosine functions which converge to that function:

$$f(x) = \sum_{n=0}^{\infty} \{a_n \cos(nx) + b_n \sin(nx)\}$$

The average monthly streamflow has a periodic form because it varies from the January to December values, then the next value would be January's again a period of a year). This periodic nature suggests that a Fourier series is a natural solution.

Several methods can be proposed to estimate the amplitude and phase of seasonal effects. Perhaps the simplest strategy is to calculate amplitude and phase using the trigonometric functions as:

$$f(x)=a_o+ \frac{A}{2}\sin[t+(F+\frac{p}{2})]$$

where F is the phase in radians.

Using a standard trigonometric identity, we can re-express the function as:

$$f(x)=a_o+ \frac{A}{2}\cos(F+\frac{p}{2})\sin(t)+ \frac{A}{2}\sin(F+\frac{p}{2})\cos(t)$$

which, setting:

$$\mathbf{b}=\frac{A}{2}\cos(F+\frac{p}{2}) \qquad\qquad \mathbf{c}=\frac{A}{2}\sin(F+\frac{p}{2})$$

can be expressed as the standard regression equation:

$$f(x)=a_o +b\sin(t) +c\cos(t)$$

Values of the phase and amplitude can be obtained from the regression coefficients using the expression:

$$F+\frac{p}{2}=\arctan(c/b) \qquad\qquad A=[2b/\cos(F+\frac{p}{2})]$$

If the sign of the coefficients b and c are the same, then F must be negative so that the peak amplitude is prior to December 30.

If one coefficient is positive, and the other negative, then the peak amplitude is after December 30, in the Spring of the year.

The phase, F, will be expressed in radians, and can be positive or negative. Note that:

- F=0 corresponds to peak occurrence at December 30.
- F=π corresponds to peak occurrence at Julian day of 182.5.

To convert the phase to a date where the amplitude peaks, we first express the phase as a Julian date via the expression:

$$F^*= \text{Phase(Julian days)} = \text{INT}(365.25\frac{F}{2p})$$

where INT: indicates the integer part of the expression.

4 Presentation of the case study

4.1 Case Study.

Ideally, a detection and attribution study requires long records of observed data for climate elements that have the potential to show large climate change signals relative to natural variability.

It is also necessary that the observing system has sufficient coverage so that the main features of natural variability and climate change can be identified and monitored.

The quality of observed data is a vital factor. Homogeneous data series are required with careful adjustments to account for changes in observing system technologies and observing practices.

Estimates of observed data uncertainties due to instrument errors or variations in data coverage are included in some recent detection and attribution studies.

The following data has been analysed within the present study.

- The base network containing 53 currently operating streamflow gauging sites in Switzerland (see **Appendix 1**: Switzerland Map) with continuous records which are not affected by anthropogenic influences and are independent in space from the Swiss Reference Hydrometric Network (SRHN) containing 231 stream-flow gauging sites (Pfaundler 2001).
- Basin attributes of the base network sites, containing areal, topographic, geological, soil and land-use information. Annual maximum daily peak flow (1931-2000) and date of annual peak flow (most of data available from 1955).

4.2 Period of study.

Three common periods of study were chosen for trend analysis, listed below. (Table **1**)

Period	Number of sites
1971-2000 (30 years)	53
1961-2000 (40 years)	34
1931-2000 (70 years)	16

Table 1: Number of sites for each period of study.

The spatial distribution of the gauging stations and their associated watersheds are presented in the following figures. (Figure **1**- Table **2-3-4**)

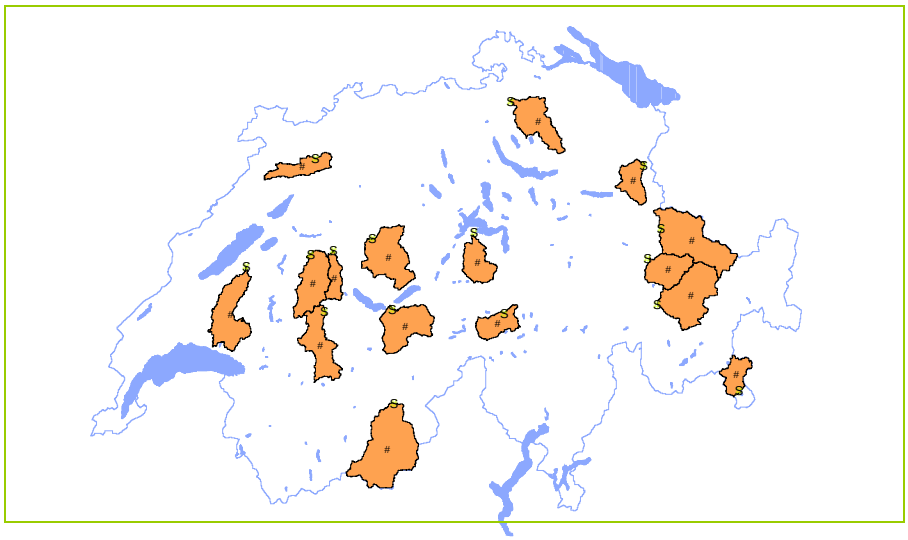

1931-2000 (16 stations)

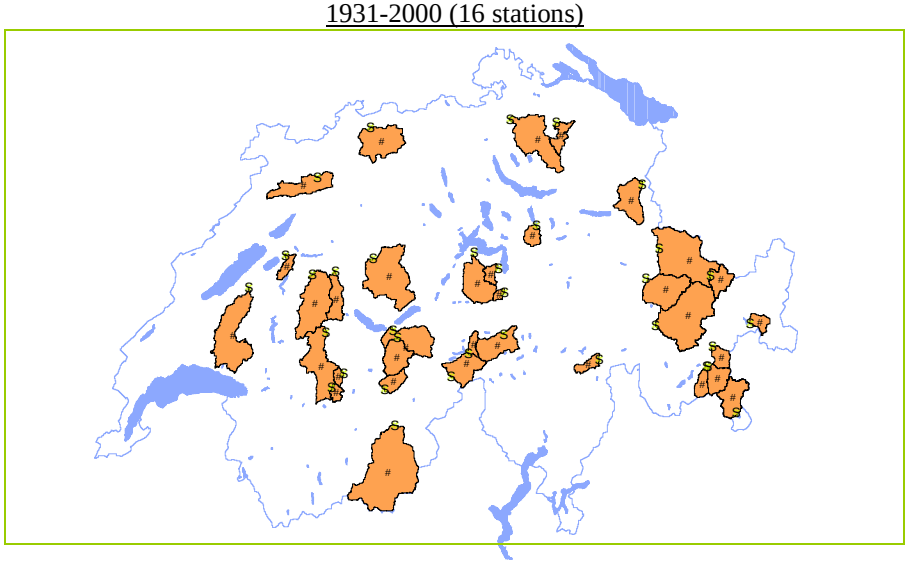

1961-2000 (34 stations)

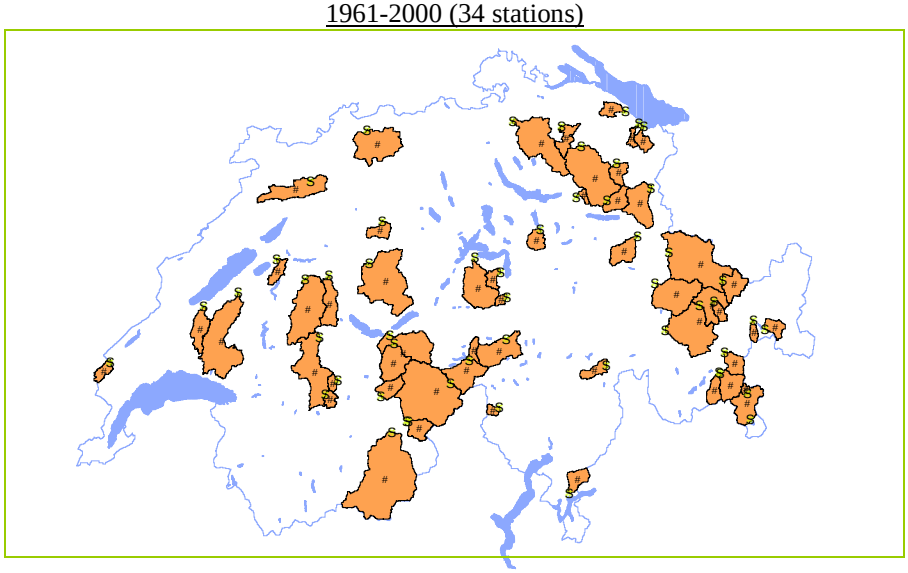

1971-2000 (53 stations)

ID	Station	River	Basin	Longitude NS	Latitude EW
152	Visp	Vispa	Rhone	124850	634150
298	Andermatt	Reuss	Reuss	166350	688170
387	Gsteig	Lütschine	Aare	168200	633130
479	Moutier	Birse	Rhein	237010	595740
549	Neftenbach	Töss	Rhein	263820	691460
614	Tiefencastel	Albula	Rhein	170145	763420
637	Oberwil	Simme	Aare	167090	600060
650	Belp. Stockmatt	Gürbe	Aare	194790	604520
698	Salez	Werdenberger Binnenkanal	Rhein	234005	756795
883	Payerne, Caserne	Broye	Aare	187320	561660
978	Thörishaus	Sense	Aare	193050	593350
1017	Chur	Plessur	Rhein	191300	758500
1064	Le Prese	Poschiavino	Adda	130520	803490
1100	Emmenmatt	Emme	Aare	200420	623610
1127	Felsenbach	Landquart	Rhein	204910	765365
1143	Buochs, Flugplatz	Engelberger Aa	Reuss	202870	673555

Table 2: Selected gauging stations for **1931-2000** analysis.

ID	Station	River	Basin	Longitude NS	Latitude EW
152	Visp	Vispa	Rhone	124850	634150
298	Andermatt	Reuss	Reuss	166350	688170
387	Gsteig	Lütschine	Aare	168200	633130
479	Moutier	Birse	Rhein	237010	595740
528	Wängi	Murg	Rhein	261720	714105
549	Neftenbach	Töss	Rhein	263820	691460
614	Tiefencastel	Albula	Rhein	170145	763420
637	Oberwil	Simme	Aare	167090	600060
650	Belp. Stockmatt	Gürbe	Aare	194790	604520
698	Salez	Werdenberger Binnenkanal	Rhein	234005	756795
716	Zweilütschinen	Weisse Lütschine	Aare	164550	635310
735	Oberried	Simme	Aare	141660	602630
740	Hinterrhein	Hinterrhein	Rhein	154680	735480
750	Adelboden	Allenbach	Aare	148300	608710
778	Pontresina	Roseggbach	Inn	151680	788780
782	Pontresina	Berninabach	Inn	151320	789440
789	Kerzers	Biberenkanal	Aare	201930	579850
792	Gletsch	Rhone	Rhone	157200	670810
793	Blatten	Lonza	Rhone	140910	629130
799	Isenthal	Grosstalbach	Reuss	196050	685500
821	Erstfeld	Alpbach	Reuss	185120	688560
822	Euthal	Minster	Limmat	215310	704425
826	Zernez	Ova da Fuorn	Inn	170790	810560
883	Payerne, Caserne	Broye	Aare	187320	561660
915	Liestal	Ergolz	Rhein	259750	622270
922	La Punt Chamues	Chamuerabach	Inn	160600	791430
933	Klosters, Auelti	Landquart	Rhein	192690	790480
939	Reckingen	Rhone (Rotten)	Rhone	146780	661910
978	Thörishaus	Sense	Aare	193050	593350
1017	Chur	Plessur	Rhein	191300	758500
1064	Le Prese	Poschiavino	Adda	130520	803490
1100	Emmenmatt	Emme	Aare	200420	623610
1127	Felsenbach	Landquart	Rhein	204910	765365
1143	Buochs, Flugplatz	Engelberger Aa	Reuss	202870	673555

Table 3: Selected gauging stations for **1961-2000** analysis.

ID	Station	River	Basin	Longitude NS	Latitude EW
152	Visp	Vispa	Rhone	124850	634150
298	Andermatt	Reuss	Reuss	166350	688170
387	Gsteig	Lütschine	Aare	168200	633130
479	Moutier	Birse	Rhein	237010	595740
528	Wängi	Murg	Rhein	261720	714105
549	Neftenbach	Töss	Rhein	263820	691460
614	Tiefencastel	Albula	Rhein	170145	763420
637	Oberwil	Simme	Aare	167090	600060
650	Belp. Stockmatt	Gürbe	Aare	194790	604520
698	Salez	Werdenberger Binnenkanal	Rhein	234005	756795
716	Zweilütschinen	Weisse Lütschine	Aare	164550	635310
735	Oberried	Simme	Aare	141660	602630
740	Hinterrhein	Hinterrhein	Rhein	154680	735480
750	Adelboden	Allenbach	Aare	148300	608710
778	Pontresina	Roseggbach	Inn	151680	788780
782	Pontresina	Berninabach	Inn	151320	789440
789	Kerzers	Biberenkanal	Aare	201930	579850
792	Gletsch	Rhone	Rhone	157200	670810
793	Blatten	Lonza	Rhone	140910	629130
799	Isenthal	Grosstalbach	Reuss	196050	685500
821	Erstfeld	Alpbach	Reuss	185120	688560
822	Euthal	Minster	Limmat	215310	704425
825	Jonschwilen	Thur	Rhein	252720	723675
826	Zernez	Ova da Fuorn	Inn	170790	810560
831	Steinach	Steinach	Rhein	262610	750760
833	, Hungerbühl	Aach	Rhein	268400	744410
834	Hundwil, Aeschentobel	Urnäsch	Rhein	244800	740170
838	Zernez	Ova da Cluozza	Inn	174830	804930
843	Pregassona	Cassarate	Ticino	97380	718010
848	Davos, Kriegsmatte	Dischmabach	Rhein	183370	786220
852	Stein, Iltishag	Thur	Rhein	228250	736020
862	Brig	Saltina	Rhone	129630	642220
863	Häberenbad	Langeten	Aare	219135	629560
864	Mels	Seez	Limmat	212510	750410
866	Brig	Rohne (Rotten)	Rhone	129700	641340
877	Davos, Frauenkirch	Landwasser	Rhein	181200	779640
879	Cavergni, Pontit	Riale di Calneggia	Ticino	135960	684970
882	Steinenbrugg	Steinenbach	Limmat	229745	721215
883	Payerne, Caserne	Broye	Aare	187320	561660
890	La Rösa	Poschiavino	Adda	142010	802120
898	La Mauguettaz	Mentue	Aare	180875	545440
908	Le Chenit,	Orbe	Aare	156305	501445
915	Liestal	Ergolz	Rhein	259750	622270
922	La Punt Chamues	Chamuerabach	Inn	160600	791430
933	Klosters, Auelti	Landquart	Rhein	192690	790480
939	Reckingen	Rhone (Rotten)	Rhone	146780	661910
978	Thörishaus	Sense	Aare	193050	593350
1017	Chur	Plessur	Rhein	191300	758500
1022	Goldach	Goldach	Rhein	261590	753190
1064	Le Prese	Poschiavino	Adda	130520	803490
1100	Emmenmatt	Emme	Aare	200420	623610
1127	Felsenbach	Landquart	Rhein	204910	765365
1143	Buochs, Flugplatz	Engelberger Aa	Reuss	202870	673555

Table 4: Selected gauging stations for **1971-2000** analysis

4.3 Basins ordering

Now, we want to try to correlate the basins and their attributes. For this reasons, we will order the basins following a new criteria:

- Basin Number 1 will be the lowest in altitude.
- Basin Number 53 will be the highest in altitude.

Our attempt is to analyze the stability of the regime and try to make a new classification on the basis of their attributes and from the results taken from the dataset analysis.

NUMBER	ID	ALTITUDE
1	833	473
2	789	539
3	915	585
4	528	648
5	549	649
6	898	682
7	831	710
8	883	722
9	863	761
10	1022	831
11	650	842
12	479	924
13	843	988
14	698	1000
15	825	1020
16	1100	1067
17	978	1069
18	834	1093
19	882	1116
20	908	1208
21	822	1336
22	852	1449
23	1143	1618
24	637	1634
25	1127	1797
26	864	1808
27	799	1815
28	750	1853.5
29	1017	1862
30	879	1989
31	862	2012
32	387	2031
33	1064	2119
34	614	2125
35	716	2152
36	821	2196
37	877	2221
38	298	2277
39	890	2290
40	939	2305
41	735	2328
42	826	2330
43	866	2335
44	933	2336
45	740	2358
46	838	2366
47	848	2371
48	922	2548
49	782	2616
50	793	2648
51	152	2655
52	792	2710
53	778	2711

4.4 Selection Criteria.

Several conditions had to be fulfilled by a selected station:

Data quality: with respect to data accuracy, only stations with continuous daily record and quality controlled were used in this project.

At these gauging stations the water level is recorded continuously. Usually four times per year the discharge measurements are executed at different stages, mostly with current meters. With these discharge measurements a stage/discharge curve is established and when necessary adjusted from time to time. Within the selected gauging stations, there are some with unstable riverbeds or aquatic weeds, which have a negative impact on the quality of the data. In small catchments it happens often that floods are very short, this translates into a lack of discharge measurements for high water levels, which are estimated by extrapolation.

No major influence by lakes or anthropogenic measures and alteration of the streamflow regime.

Only gauging stations that are not overly influenced by anthropogenic measures, like reservoirs or water diversions, were considered. The presence of major lakes within the watershed of a gauging station inhibits its selection, since the hydraulic (attenuating) effect on the magnitude of floods is too site-specific for being used for information transfer (Pfaundler, 2001). The related catchments of the selected gauging stations don't contain reservoirs or lakes that capture more than 10% of the total basin area.

Regarding the streamflow regime, three exceptions have been made in order to provide a better spatial coverage.

There are 3 stations with about 40% alteration of the streamflow regime, which were also analyzed. Nevertheless, for average and maximum streamflow, the time series are statistically satisfying.

These three stations are:

Vispa at Visp	ID 152
Reuss at Andermatt	ID 298
Albula at Tiefencastel	ID 614

Minimum sample size. The significance and accuracy of the statistical properties of streamflow series depend strongly upon the sample size. The minimum sample size of daily records has been set here to thirty years.

Independence from other sites. In some cases more than one gauging station were located along the same river.

The selection procedure made by Pfaundler (2001) has pointed out the following criteria. If two stations are situated along the same river the upstream station is selected. A downstream station is additionally selected only under the following conditions:

For A_i <50 km²	$A_j = 2\ A_i$
For 50 km² < A_i < 200 km²	$A_j = 1.5\ A_i$
For A_i > 200 km²	$A_j = 1.33\ A_i$

where A represents the basin drainage area, *i* is the upstream station and *j* is the downstream station.

These conditions offer a good compromise between the assumed independence of the station records and the quite high number of stations and allow a fair spatial distribution throughout Switzerland even for the 70 years analysis (1931-2000).

The majority of studies regarding this type of analyses have assumed that recorded streamflow series are serially independent, even though certain hydrological time series such as annual mean and annual minimum streamflow may frequently display statistically significant serial correlation.

4.5 Basin attributes.

The basin attributes were determined from several digital sources by Pfaundler (2001).(Table **5**)

Basin area [km²]. The basin area is the direct outcome of the watershed delineation. One may expect the existence of certain scale ranges, that is, ranges of basin areas within which the same flood related processes are prevalent. For instance, the larger the basin, the more important the runoff concentration; the smaller the basin, the greater the relevance of runoff generation processes (Pilgrim *et al.*, 1982).

Gravelius index K_G. It is one of the several geomorphologic indexes, which allows a comparison between several hydrographical watersheds. Defined by Gravelius (1914) K_G represents the fraction between the perimeter of the basin the perimeter of a circle having the same surface.

The Gravelius index is close to one if the shape of the basin is similar with a circle and increases with the lengthened shapes. Due to the fact that the watershed contours are

derived from (fine) raster images, K_G values are overestimated.

Mean altitude. The mean elevation of a basin is considered an indicator for the discharge regime, which is related to elevation zones. Furthermore, this attribute shows strong correlations with many other basin characteristics.

Mean slope. Features that are related to slope are runoff concentration processes, the extent of the contributing area and the runoff type.

River network density [m/km²]. The river network density is defined as the ratio between the total river network length (m) and the basin area (km²) and is considered an indicator for the runoff disposition, the extent of the contributing area and the runoff concentration. River network density is a relative measurement for comparison among basins, due to its dependency on the underlying map scale.

The higher the scale, the more ramified the network, and the longer the total network length (Pfaundler, 2001). It can be calculated directly from the topographic map, or it may be extracted from a digital elevation model (Tarboton *et al*., 1991). The river network density was computed from the digital river network of Switzerland contained in the topographic maps 1:25'000.

Mean soil depth [cm]. For determining the hydrologic soil types, the digital soil map and the digital geotechnical map have been used as information basis. The digital soil map of Switzerland (GEOSTAT, 1997) is based on a paper map with scale 1:200'000. This map contains generalizations and aggregation of information, but has a good number of soil classification units (146), each of them characterized by a number of soil properties; it provides information about soil depth and permeability of the single classification units.

Percentage of glacier coverage [%]. Since many basins in the alpine zone are glacierized, an attribute is necessary that reflects the importance of glacier related processes in a basin. For this purpose, the percentage of glacier coverage has been computed for the analyzed basins. The underlying information on glacierisation stems from the digital geotechnical map of Switzerland (GEOSTAT, 1997) derived from a 1:200'000 map with containing 30 classification units.

Percentage of rock coverage [%]. It is relevant especially for the alpine regions of Switzerland, and it indicates low infiltration and quick runoff.

Mean annual precipitation [mm/year]. The mean annual precipitation is an indicator for the system condition, like a climatic or wetness index. The annual value conceals the inter-annual distribution.

ID	Area km²	K-Gravelius	Mean Altitude	Mean Slope	River Density	Mean Soil Depth	Rock Cover	Glacier Cover	Mean Annual Precip.
152	778	1.835	2655	29	1072	13	26.5	29.3	737
298	192	1.949	2277	26.1	2367	20	30.8	5.5	1636
387	379	1.896	2031	30.1	1553	20	26.6	16.6	1367
479	183	2.537	924	15.1	918	56	0.3	0	1284
528	78.9	2.772	648	11.3	2095	86	0.3	0	1277
549	342	2.258	649	11.6	2522	82	0.2	0	1251
614	529	1.906	2125	27.1	1511	22	23.1	1.2	994
637	344	2.576	1634	23.2	1847	33	9.9	3.4	1408
650	124	2.333	842	12.2	1943	76	0.9	0	1224
698	180	1.896	1000	17.2	2138	50	4.3	0	1403
716	164	1.676	2152	31.8	1268	17	33.3	16.5	1346
735	35.7	1.799	2328	23.8	1069	10	36.6	32.1	1311
740	53.7	2.058	2358	27.8	2500	19	37.6	19.3	1530
750	28.8	1.593	1853.5	25.9	2380	28.8	14.6	0	1535
778	66.5	1.742	2710	28.3	1192	11	37.1	32.6	948
782	107	1.754	2616	25.4	1290	15	38.1	21.1	1110
789	50.1	2.29	539	3.6	1032	98	0	0	1007
792	38.9	1.961	2710	22.8	828	10	34.7	45.7	1737
793	77.8	1.753	2648	29.6	1256	10	37.5	32.6	1098
799	43.9	1.916	1815	30.9	1006	19	24.7	9.7	1488
821	20.6	1.644	2196	33.6	713	10	57	19.7	1392
822	59.2	1.549	1336	19	4121	39	2.6	0	2151
825	493	1.991	1020	17.9	2854	65	3.4	0	1723
826	55.3	1.804	2330	25.3	1304	22	31.8	0	865
831	24.2	2.707	710	9.1	2215	62	0.3	0	1343
833	48.5	1.979	473	2.6	1406	93	0	0	1011
834	64.5	1.779	1093	17.7	3074	68	3	0	1904
838	26.9	1.626	2366	33.8	708	10	47.2	2.6	816
843	73.9	1.7	988	23.8	3729	34	0.3	0	1816
848	43.3	1.691	2371	26.9	1732	17	34.7	2.7	990
852	84	1.788	1449	22.8	1175	35	9.5	0	1901
862	77.7	1.744	2012	29.3	1977	27	20.3	7.2	845
863	59.9	1.886	761	10	1647	97	0	0	1338
864	105	1.807	1808	29.9	2574	29	21.9	0.3	1396
866	913	2.185	2335	27	1524	19	26.8	22.7	1152
877	183	1.861	2221	24.7	2098	21	23.7	0.8	1038
879	25	1.484	1989	34.2	1058	16	57.6	0	1807
882	19.1	1.933	1116	21.1	3769	56	1.4	0	1714
883	392	2.686	722	7.3	1693	90	0.1	0	1215
890	14.1	1.773	2290	24.3	1772	25	15.9	0	1455
898	105	2.303	682	5.9	1463	98	0	0	1106
908	44.4	2.18	1208	9.2	523	46	0.1	0	1585
915	261	1.905	585	13.6	1223	71	0.1	0	1067
922	73.3	1.624	2548	27.4	1222	17	33.2	0	927
933	112	1.887	2336	29.1	1342	14	38.5	10.2	1073
939	215	2.124	2305	26	1697	20	28	15.8	1487
978	352	2.079	1069	15.8	2844	71	3.3	0	1337
1017	263	1.715	1862	24.4	1729	32	12.9	0	1096
1022	49.8	2.097	831	13.8	2907	81	0	0	1437
1064	169	1.925	2119	27	1731	22	21.4	4.6	1214
1100	443	2.06	1067	18.7	3165	70	3.1	0	1478
1127	616	2.19	1797	25.5	1950	32	14.6	1.7	1194
1143	227	1.865	1618	29	1352	24	19.4	4.3	1474

Table 5: Basin Attributes

5. Discussion of Results

5.1 Streamflow analysis.

For the 53 basins we have calculated the variables and the parameters described in the previous section.

For each basin diagrams have been plotted:

- Monthly streamflow time series
- Time series of annual streamflow variance of daily data
- Time series of the Julian day in which the first and second maximum daily streamflow occur
- Time series of the Julian day in which the first, second and third minimum daily streamflow occur
- Time series of the first and second maximum month of the year in which streamflow occur
- Time series of the first, second and third minimum month of the year in which streamflow occur
- Time series of the annual estimate of the Fourier series phase and amplitude
- Time series of the streamflow average regime interpolated by the Fourier series
- Time series of the Informational Entropy related to maximum monthly streamflow
- Time series of the Informational Entropy related to minimum monthly streamflow

5.2 Annual Daily Streamflow

The spatial distribution of changes in annual and seasonal mean, minimum and maximum daily streamflow for the period 1971-2000 are listed in the Table **6**.

	ANNUAL			WINTER			SPRING			SUMMER			AUTUMN			
ID	**Mean**	**Min**	**Max**	**Mean**	**Min**	**Max**	**Mean**	**Min**	**Max**	**Mean**	**Min**	**Max**	**Mean**	**Min**	**Max**
152	17.37	2.76	78.37	17.29	4.00	50.23	23.12	5.86	66.96	15.02	3.79	47.56	14.07	3.28	35.20
298	7.11	1.36	53.89	2.03	1.46	3.64	5.91	1.43	22.68	14.11	6.15	44.25	6.30	2.68	36.95
387	18.77	2.34	84.23	4.17	2.53	15.94	15.26	3.40	48.88	41.81	20.41	81.58	13.50	4.11	49.96
479	3.24	0.85	23.42	3.88	1.36	17.63	4.11	1.85	15.30	2.59	1.07	13.61	2.37	0.91	11.24
528	1.84	0.39	15.21	2.28	0.68	11.73	2.04	0.69	9.53	1.54	0.46	9.96	1.50	0.48	8.99
549	7.98	1.91	77.47	9.07	2.87	49.41	9.34	3.14	49.31	7.17	2.24	49.56	6.33	2.12	36.92
614	14.71	4.24	60.16	5.66	4.43	7.59	12.25	4.52	38.45	28.28	14.25	58.07	12.46	7.09	30.08
637	12.04	2.88	54.63	6.20	3.22	29.92	15.14	4.43	40.09	17.93	9.39	43.00	8.76	4.11	33.01
650	2.67	0.80	18.53	2.57	0.99	12.64	3.16	1.40	10.92	2.82	1.04	13.57	2.14	0.91	11.39
698	7.85	0.78	45.55	6.14	0.86	27.55	8.63	0.85	26.67	9.91	1.65	37.39	6.67	1.31	25.51
716	8.15	3.00	37.93	1.65	3.42	5.04	6.09	4.29	20.90	18.82	4.80	36.89	5.87	3.55	21.60
735	2.09	1.00	11.14	0.31	1.06	0.97	1.06	1.31	3.88	5.34	8.85	10.95	1.59	1.86	5.88
740	3.37	0.18	35.27	0.50	0.19	0.90	2.18	0.20	11.04	7.91	1.84	30.09	2.83	0.42	24.55
750	1.21	0.30	6.48	0.43	0.37	1.61	1.81	0.36	5.77	1.81	2.84	5.68	0.75	0.71	3.01
778	2.85	0.24	19.61	0.21	0.27	0.41	0.99	0.33	5.25	7.81	0.54	18.40	2.31	0.34	12.73
782	4.56	0.11	34.94	0.42	0.12	0.71	2.68	0.12	14.39	11.60	2.45	30.94	3.43	0.43	21.41
789	0.55	0.28	4.73	0.70	0.29	3.50	0.62	0.32	2.58	0.43	4.50	2.08	0.47	0.74	2.99
792	2.81	0.18	15.00	0.32	0.31	0.68	0.82	0.31	4.10	7.72	0.20	14.87	2.33	0.21	8.58
793	4.76	0.21	24.82	0.65	0.22	1.07	2.31	0.23	9.38	12.22	2.23	24.21	3.77	0.46	13.82
799	1.72	0.46	7.47	0.68	0.48	2.68	2.04	0.48	5.54	2.87	4.05	6.93	1.29	0.95	4.05
821	1.63	0.38	10.37	0.18	0.41	1.14	1.07	0.51	4.33	4.05	1.34	10.24	1.18	0.58	5.65
822	3.10	0.09	31.67	1.44	0.10	14.76	4.71	0.13	19.29	3.97	1.45	26.72	2.20	0.20	18.65
825	20.83	0.27	202.2	16.71	0.38	135.6	27.14	0.69	128.8	23.02	0.44	158.5	16.34	0.33	111.0
826	1.05	2.46	5.18	0.45	3.52	0.59	1.07	6.89	4.17	1.79	4.39	4.36	0.88	3.01	2.27
831	0.80	0.30	8.27	0.76	0.34	3.85	0.88	0.34	5.15	0.83	0.78	6.75	0.71	0.57	4.91
833	0.75	0.24	10.48	0.96	0.30	6.62	0.80	0.30	5.94	0.62	0.26	6.27	0.63	0.27	5.61
834	2.82	0.10	28.02	2.14	0.23	16.86	3.65	0.19	18.16	3.15	0.11	24.17	2.33	0.13	16.39
838	0.79	0.30	5.67	0.20	0.43	0.29	0.69	0.75	3.11	1.66	0.49	5.04	0.59	0.40	3.40
843	2.58	0.14	22.88	1.40	0.16	5.16	3.50	0.14	14.01	2.61	0.61	14.05	2.81	0.26	15.39
848	1.70	0.51	7.95	0.45	0.72	0.66	1.27	1.05	5.18	3.71	0.72	7.83	1.35	0.73	3.69
852	3.88	0.29	35.86	1.67	0.32	17.76	5.22	0.30	19.85	5.91	1.81	28.22	2.67	0.64	17.99
862	2.42	0.33	16.47	1.04	0.42	1.64	1.76	0.80	6.43	4.75	1.14	12.04	2.11	0.42	11.11
863	1.25	0.65	7.86	1.37	0.80	5.52	1.46	0.68	4.45	1.16	1.94	4.68	1.02	1.11	3.94
864	2.83	0.56	16.90	1.09	0.75	4.64	3.73	0.83	11.23	4.39	0.65	15.07	1.98	0.60	8.48
866	42.18	0.57	202.8	9.04	0.60	14.98	23.29	0.92	87.51	101.5	1.45	183.3	34.11	0.81	132.3
877	5.44	5.99	24.78	1.53	6.51	2.76	4.16	6.69	14.81	11.64	36.62	24.27	4.35	10.42	10.98
879	1.40	0.97	21.95	0.24	1.06	0.44	1.40	1.06	8.49	2.50	5.27	12.54	1.45	2.14	15.13
882	1.00	0.14	11.00	0.58	0.15	5.27	1.45	0.19	6.57	1.15	0.71	9.77	0.77	0.36	6.09
883	8.18	0.07	91.13	11.17	0.11	78.20	9.46	0.23	52.52	5.16	0.11	35.65	7.04	0.09	50.04
890	0.57	1.36	4.20	0.20	2.71	0.30	0.60	3.17	2.63	0.93	1.65	3.07	0.52	1.59	2.68
898	1.59	0.13	15.81	2.36	0.14	14.03	1.78	0.15	9.07	0.95	0.38	5.27	1.29	0.25	8.32
908	0.96	0.30	7.27	1.13	0.76	5.76	1.30	0.73	5.35	0.51	0.37	2.28	0.89	0.36	4.21
915	3.70	0.07	37.56	5.06	0.23	26.82	4.52	0.27	25.84	2.60	0.10	20.47	2.64	0.14	18.29
922	2.19	0.40	11.69	0.74	1.07	1.00	1.43	1.16	5.75	4.62	0.53	11.27	1.93	0.48	5.57
933	5.70	0.53	24.75	1.01	0.58	1.67	4.10	0.54	16.32	13.48	2.19	24.01	4.07	1.00	13.04
939	10.02	0.67	52.55	2.43	0.71	4.15	7.09	0.72	25.58	22.61	6.23	48.71	7.78	1.50	31.46
978	8.87	1.75	73.20	7.31	1.85	44.90	11.93	1.96	48.69	9.20	10.62	54.84	7.00	3.11	44.72
1017	7.87	1.92	34.39	2.71	2.30	4.91	9.35	3.91	26.01	13.36	2.54	31.97	5.94	2.14	17.89
1022	1.38	1.71	17.67	1.31	1.95	7.49	1.61	2.28	9.69	1.44	5.19	15.13	1.16	3.13	8.91
1064	5.96	0.20	33.68	2.78	0.34	4.56	4.82	0.36	15.87	10.49	0.25	27.36	5.69	0.26	22.02
1100	11.90	1.13	110.9	9.58	1.23	65.45	16.61	1.27	67.39	12.62	5.23	87.23	8.65	2.28	53.05
1127	24.25	1.83	114.3	8.87	2.58	21.76	28.90	4.83	83.34	42.67	2.43	110.3	16.19	2.08	53.69
1143	12.32	5.80	52.56	4.70	6.29	13.69	11.33	8.06	32.65	23.70	17.29	51.30	9.37	8.23	28.13

Table 6: Spatial distribution of changes in annual and seasonal mean, minimum and maximum daily streamflow.

5.3 Fourier Analysis.

The monthly data derived from the data base, are analyzed with the Fourier analysis described in the previous chapter.

Hydrologic series defined at time intervals smaller than a year (such as monthly series) generally exhibit distinct seasonal (or periodic) patterns.

These result from the annual revolution of the Earth around the sun which produces the annual cycle in most hydrologic processes.

Seasonal or periodic patterns of hydrologic series translate into statistical characteristics which vary within the year.

To remove the seasonality in the mean, we consider the series: $y_t - \overline{y_t}$

where:

- $\overline{y_t}$ is the monthly mean for January, February,…. December.
- *t* is the monthly index.

We present the results of the Fourier analysis of the original data series. (Figure **2-3-4-5-6;** Table **7**)

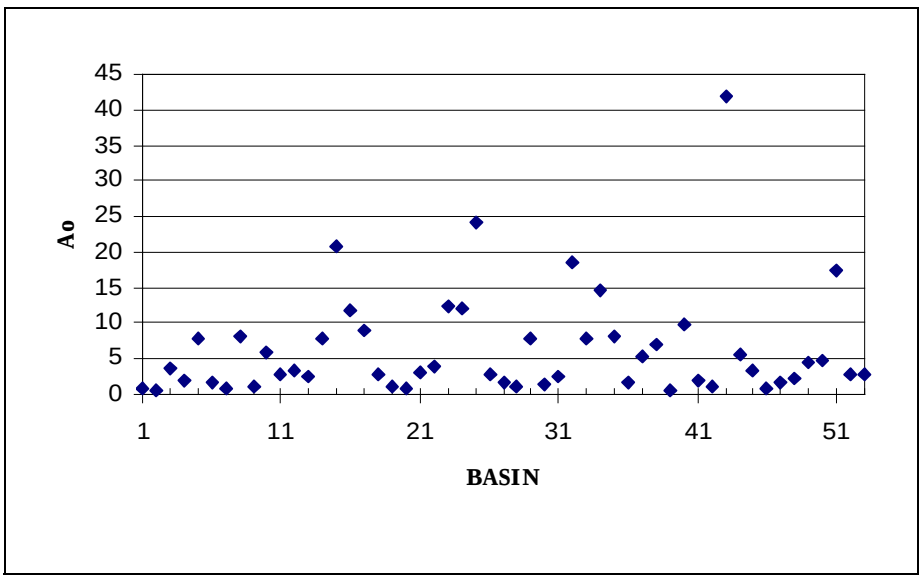

Figure 2: Ao coefficient for the 53 basins. (Period 1971-2000)

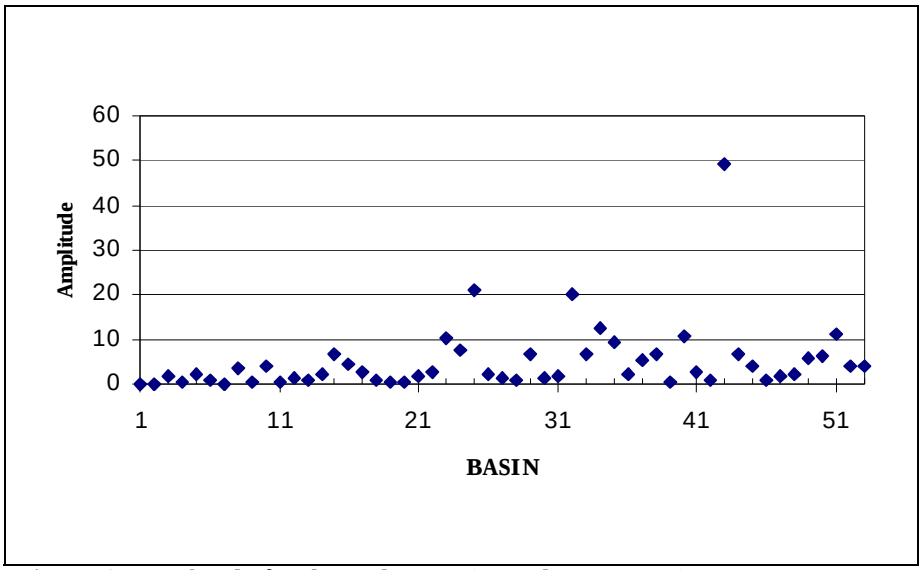

Figure 3: Amplitude for the 53 basins. (Period 1971-2000)

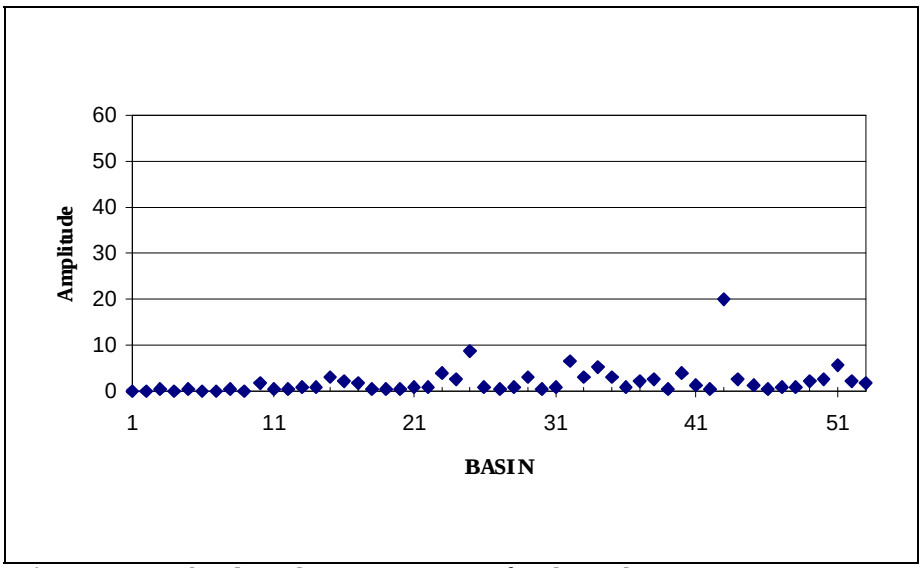

Figure 4: Amplitude with two Harmonics for the 53 basins.

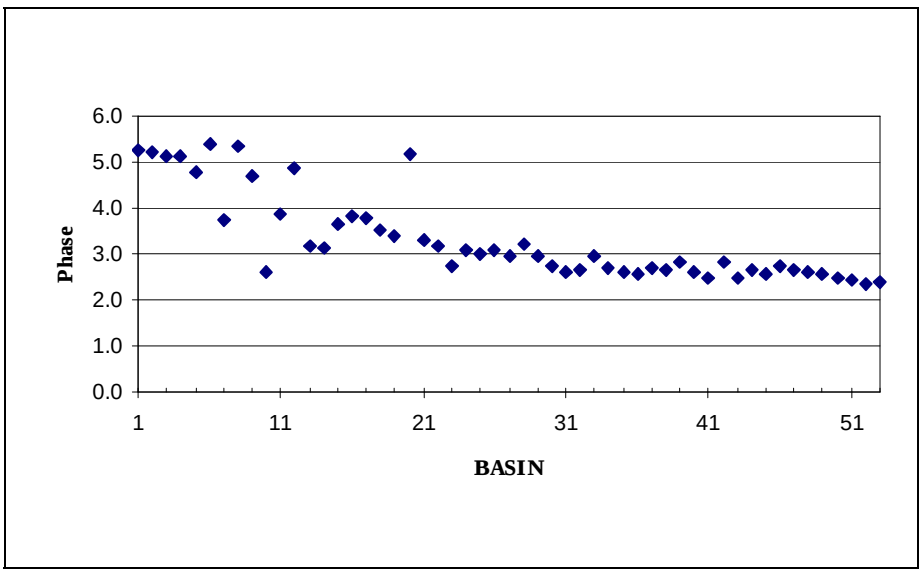

Figure 5: Phase for the 53 basins. (Period 1971-2000)

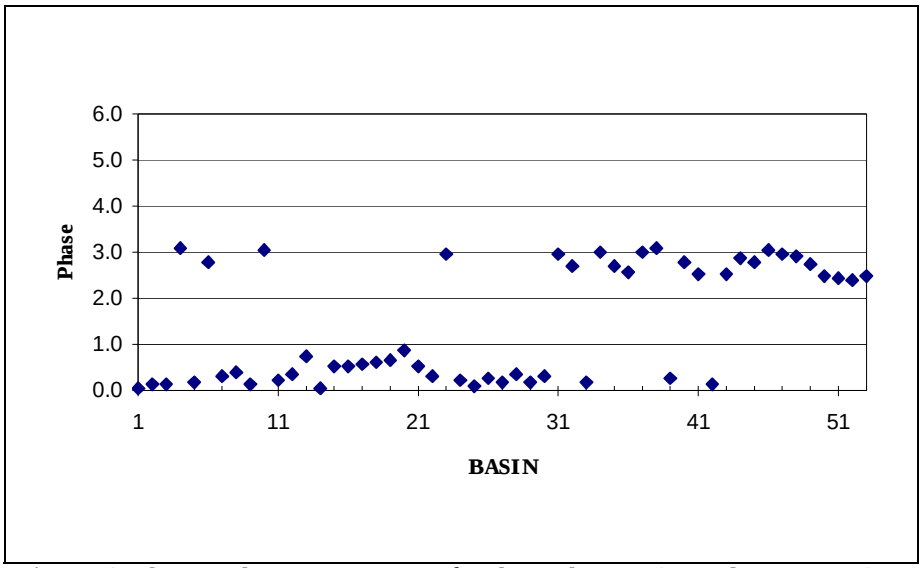

Figure 6: Phase with two Harmonics for the 53 basins. (Period 1971-2000)

Because of the basins different physiographic characteristics, it is necessary to apply a data dimensionless to make them comparable by taking the ratio: $\frac{\overline{y_t}}{y_t}$

where:

- $\overline{y_t}$ is the monthly mean for January, February,…. December.
- t is the monthly index.

We present the results of the Fourier analysis of the dimensionless data series in Figure **7-8-9**; Table **8**.

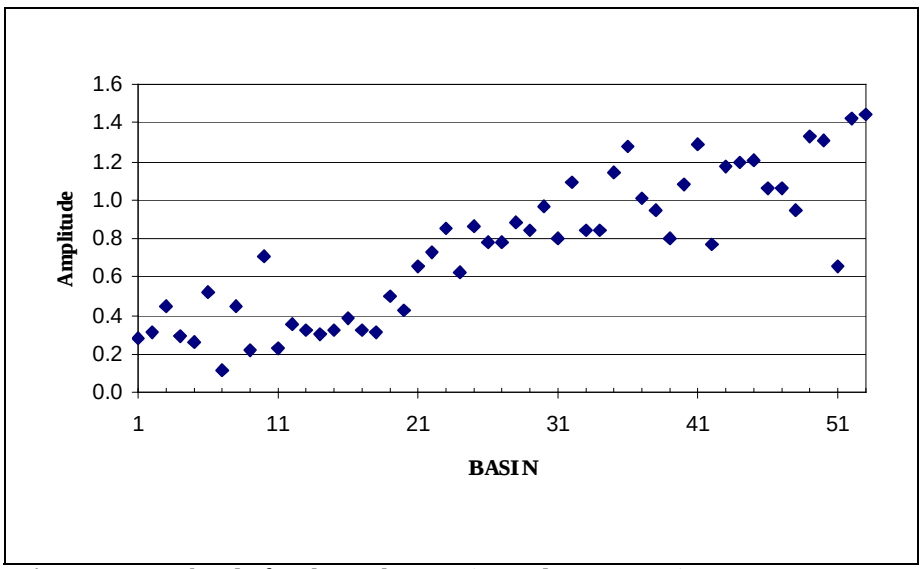

Figure 7: Amplitude for the 53 basins. (Period 1971-2000)

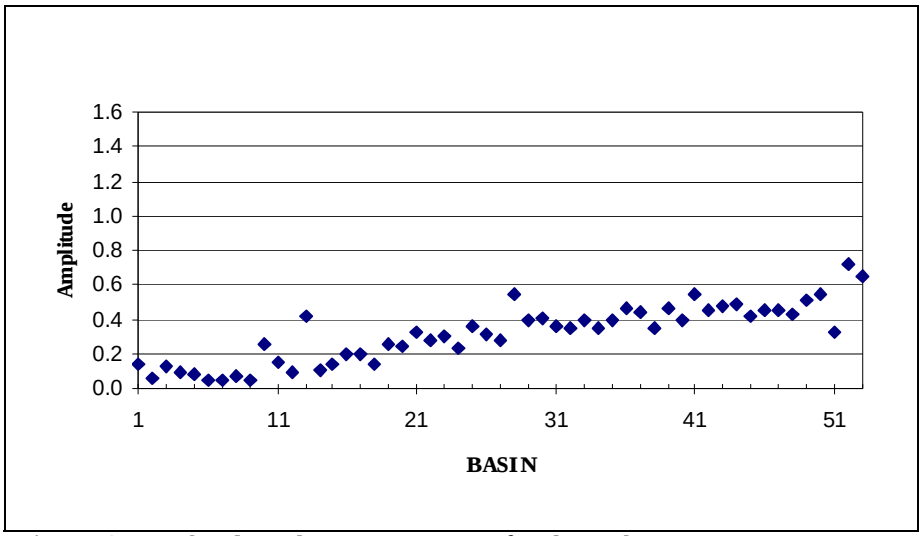

Figure 8: Amplitude with two Harmonics for the 53 basins.

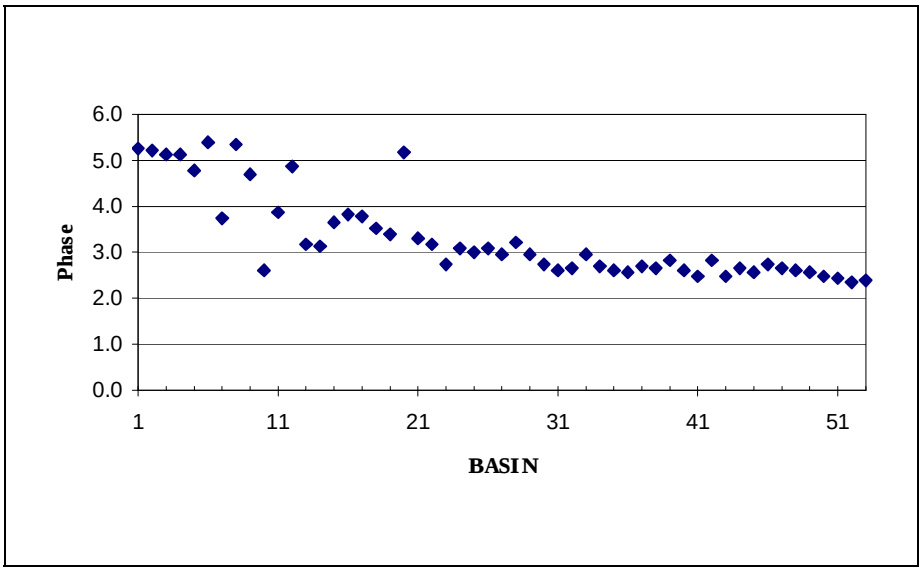

Figure 9: Phase for the 53 basins. (Period 1971-2000)

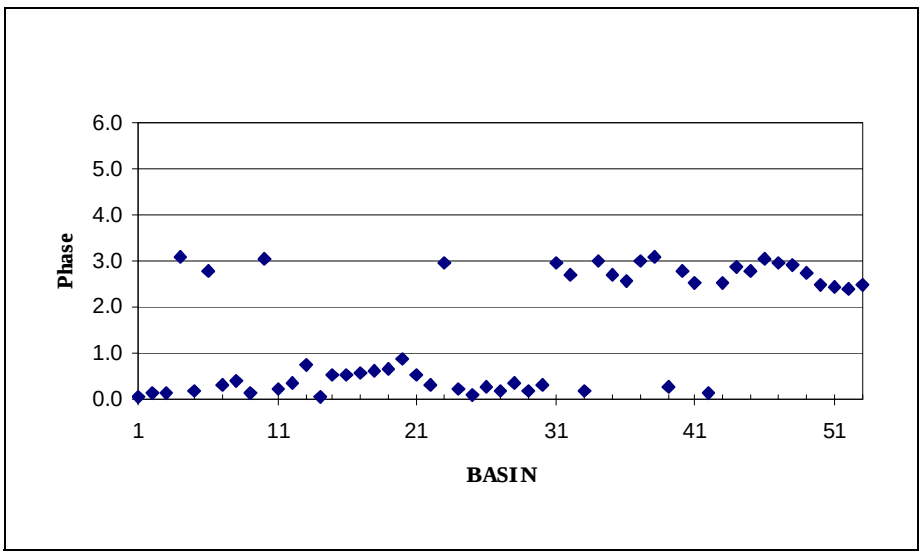

Figure 10: Phase with two Harmonics for the 53 basins. (Period 1971-2000)

Basin	Ao	Amplitude	Phase	Amplitude with two Harmonics	Phase with two Harmonics
1	0.75	0.21	5.25	0.10	0.06
2	0.56	0.18	5.21	0.03	0.13
3	3.71	1.66	5.11	0.49	0.15
4	1.84	0.53	5.15	0.16	3.11
5	7.99	2.06	4.79	0.65	0.15
6	1.59	0.83	5.39	0.08	2.77
7	0.80	0.09	3.75	0.03	0.29
8	8.22	3.69	5.36	0.53	0.41
9	1.25	0.28	4.68	0.06	0.14
10	5.95	4.23	2.59	1.53	3.03
11	2.68	0.61	3.88	0.40	0.23
12	3.24	1.16	4.86	0.30	0.35
13	2.59	0.84	3.17	1.08	0.72
14	7.84	2.35	3.12	0.79	0.06
15	20.83	6.77	3.65	2.93	0.50
16	11.89	4.58	3.81	2.30	0.54
17	8.88	2.87	3.78	1.72	0.55
18	2.82	0.89	3.53	0.40	0.62
19	0.99	0.49	3.41	0.25	0.67
20	0.96	0.41	5.19	0.23	0.85
21	3.09	2.01	3.33	0.98	0.54
22	3.87	2.82	3.16	1.08	0.29
23	12.28	10.45	2.75	3.71	2.94
24	12.02	7.55	3.09	2.76	0.23
25	24.21	20.86	3.02	8.67	0.10
26	2.80	2.17	3.10	0.89	0.28
27	1.72	1.33	2.95	0.48	0.16
28	1.20	1.06	3.23	0.66	0.34
29	7.86	6.62	2.98	3.07	0.19
30	1.40	1.34	2.72	0.56	0.29
31	2.42	1.94	2.60	0.86	2.94
32	18.68	20.31	2.65	6.53	2.69
33	7.86	6.62	2.98	3.07	0.19
34	14.68	12.40	2.69	5.07	3.02
35	8.10	9.23	2.62	3.22	2.69
36	1.62	2.08	2.57	0.75	2.58
37	5.42	5.49	2.68	2.37	2.98
38	7.09	6.70	2.66	2.43	3.07
39	0.57	0.45	2.83	0.26	0.25
40	9.98	10.81	2.61	3.99	2.77
41	2.07	2.66	2.49	1.14	2.53
42	1.05	0.80	2.84	0.47	0.13
43	41.98	49.09	2.49	19.92	2.53
44	5.67	6.78	2.67	2.73	2.85
45	3.35	4.05	2.58	1.39	2.79
46	0.78	0.83	2.76	0.36	3.06
47	1.69	1.79	2.67	0.77	2.96
48	2.18	2.06	2.60	0.93	2.93
49	4.53	6.02	2.59	2.30	2.75
50	4.73	6.19	2.46	2.60	2.50
51	17.31	11.27	2.43	5.60	2.45
52	2.79	3.98	2.37	2.02	2.39
53	2.83	4.08	2.41	1.85	2.46

Table 7: Results of the original series.

Basin	Amplitude	Phase	Amplitude with two Harmonics	Phase with two Harmonics
1	0.28	5.25	0.14	0.06
2	0.32	5.21	0.06	0.13
3	0.45	5.11	0.13	0.15
4	0.29	5.15	0.09	3.11
5	0.26	4.79	0.08	0.15
6	0.52	5.39	0.05	2.77
7	0.11	3.75	0.04	0.29
8	0.45	5.36	0.06	0.41
9	0.22	4.68	0.05	0.14
10	0.71	2.59	0.26	3.03
11	0.23	3.88	0.15	0.23
12	0.36	4.86	0.09	0.35
13	0.33	3.17	0.42	0.72
14	0.30	3.12	0.10	0.06
15	0.33	3.65	0.14	0.50
16	0.39	3.81	0.19	0.54
17	0.32	3.78	0.19	0.55
18	0.32	3.53	0.14	0.62
19	0.50	3.41	0.25	0.67
20	0.43	5.19	0.24	0.85
21	0.65	3.33	0.32	0.54
22	0.73	3.16	0.28	0.29
23	0.85	2.75	0.30	2.94
24	0.63	3.09	0.23	0.23
25	0.86	3.02	0.36	0.10
26	0.77	3.10	0.32	0.28
27	0.77	2.95	0.28	0.16
28	0.88	3.23	0.55	0.34
29	0.84	2.98	0.39	0.19
30	0.96	2.72	0.40	0.29
31	0.80	2.60	0.36	2.94
32	1.09	2.65	0.35	2.69
33	0.84	2.98	0.39	0.19
34	0.85	2.69	0.35	3.02
35	1.14	2.62	0.40	2.69
36	1.28	2.57	0.46	2.58
37	1.01	2.68	0.44	2.98
38	0.94	2.66	0.34	3.07
39	0.80	2.83	0.47	0.25
40	1.08	2.61	0.40	2.77
41	1.29	2.49	0.55	2.53
42	0.77	2.84	0.45	0.13
43	1.17	2.49	0.47	2.53
44	1.20	2.67	0.48	2.85
45	1.21	2.58	0.41	2.79
46	1.06	2.76	0.46	3.06
47	1.06	2.67	0.45	2.96
48	0.95	2.60	0.43	2.93
49	1.33	2.59	0.51	2.75
50	1.31	2.46	0.55	2.50
51	0.65	2.43	0.32	2.45
52	1.42	2.37	0.72	2.39
53	1.44	2.41	0.65	2.46

Table 8: Results of the dimensionless series.

The results obtained from phase analysis with an harmonic point out how is strictly correlated to the basin physiographic characteristics.

As shown by graphs, it is evident that the phase is a quantity that grows less when altitude increase and therefore when rock and ice coverage percentage increases. On the contrary the phase calculated with two harmonics results very variable.

This variability is not justified by a substantial variation of the curves fitting.

The amplitude with an harmonic grows up when altitude increases, so with the passage from alpine regime basins to snow-glacial regime basins. As well as for the phase, also amplitude with two harmonics is not much significant for the kind of analysis done, because it is the result of a curves fitting and so not easily correlate to the basins characteristics.

It is also pointed out that, though R^2 values were better when using two harmonics, the use of a single harmonic gives a good curves fitting.

5.4 Informational Entropy.

We can plot the results in the Switzerland map to see the spatial distributions of the maximum and minimum monthly streamflow stability.(Figure **11-12**; Table **9**)

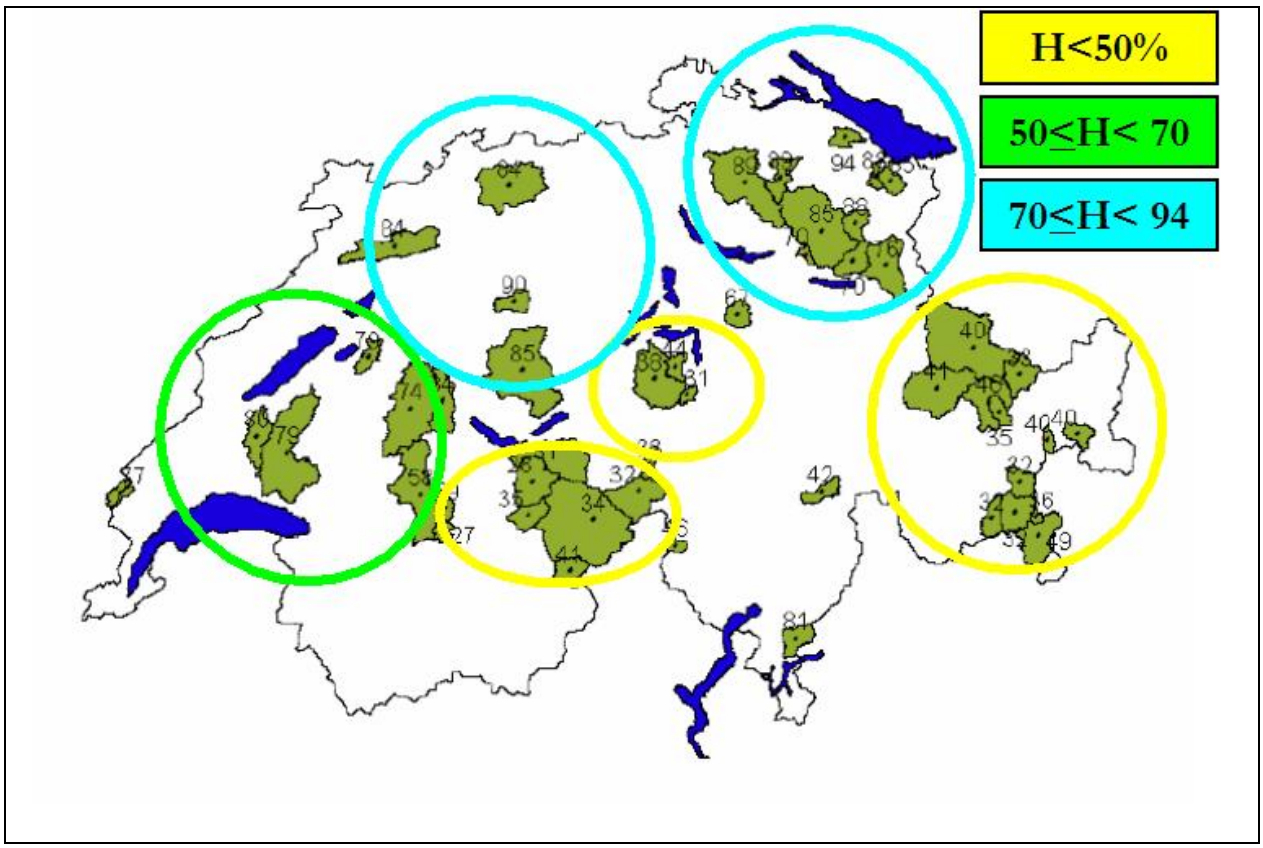

Figure 11: Spatial distribution of stability of streamflow maxima.

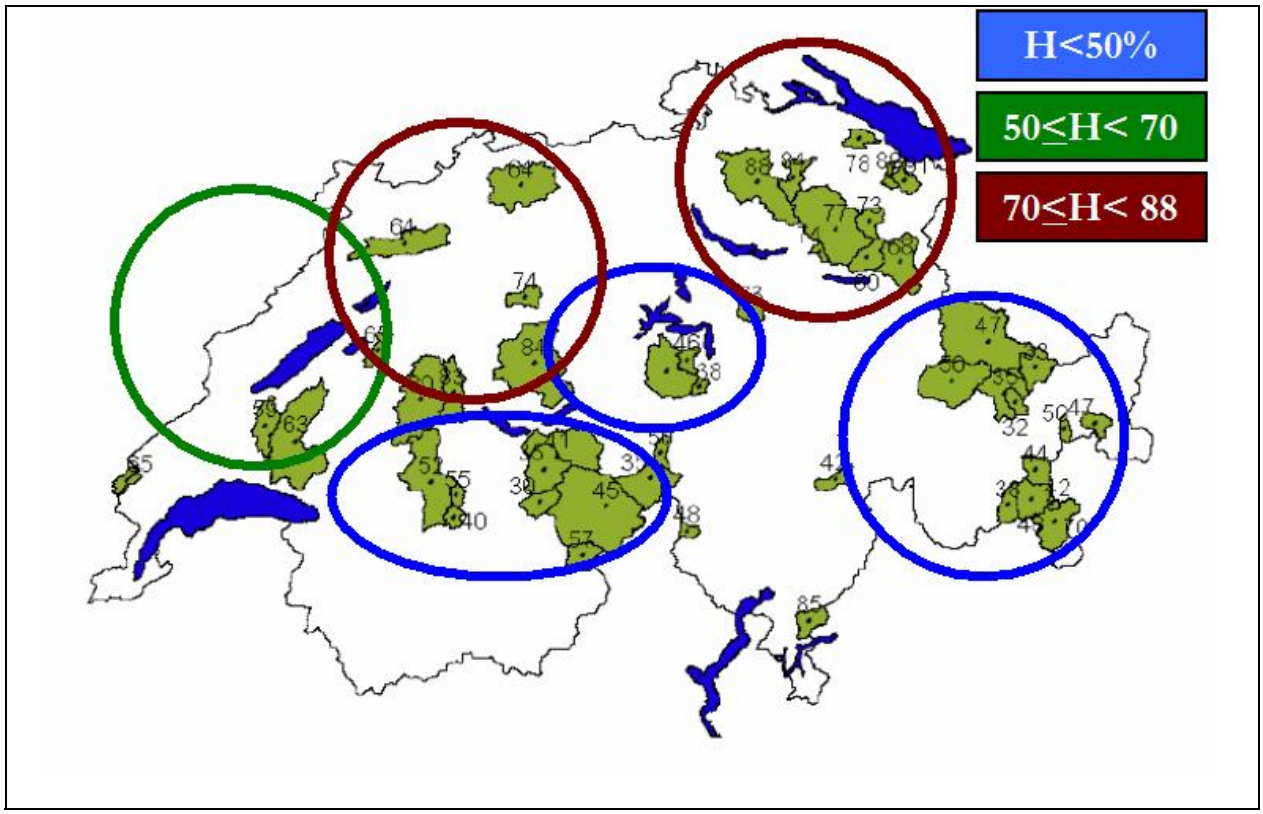

Figure 12: Spatial distribution of stability of streamflow minima.

If we plot on a graph this indicator and all the basins in altitude order, we can see if the altitude and the stability of the regime are correlated (Figure 13, Table **10**).

As shown by the graph, it is evident that the entropy is a quantity that grows less when altitude increase and therefore when rock and ice coverage percentage increases.

The index is an effective tool of analysis in order to distinguish the basins according to the values of the considered quantity.

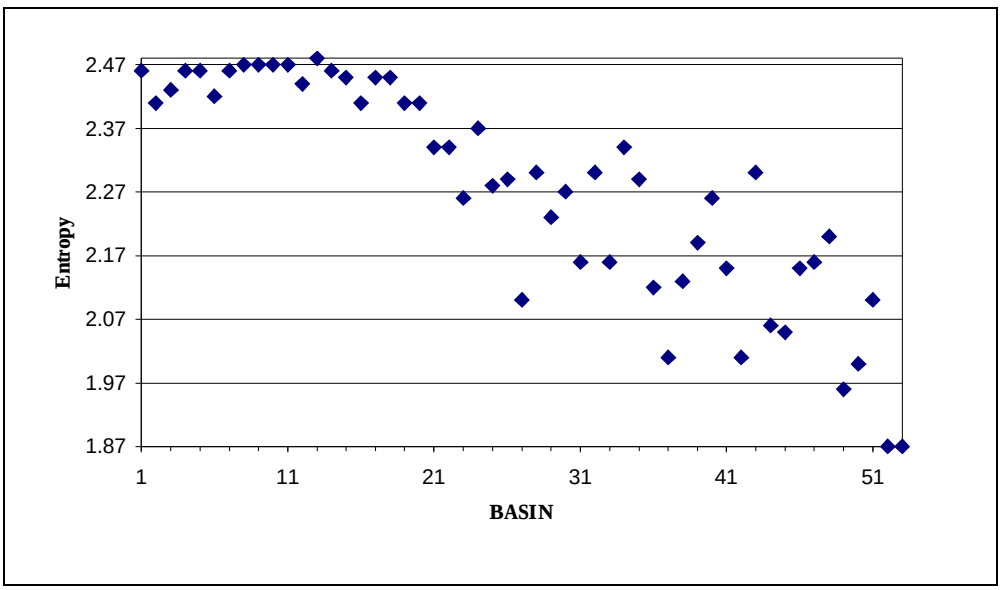

Figure 13: Informational Entropy for the 53 basins. (Period 1971-2000)

N° BASIN	Entropy of maxima	Entropy of minima
1	0.94	0.78
2	0.79	0.65
3	0.84	0.64
4	0.89	0.84
5	0.89	0.88
6	0.8	0.59
7	0.88	0.89
8	0.79	0.63
9	0.9	0.74
10	0.85	0.91
11	0.84	0.83
12	0.84	0.64
13	0.81	0.85
14	0.76	0.68
15	0.85	0.77
16	0.85	0.84
17	0.74	0.8
18	0.88	0.73
19	0.7	0.74
20	0.77	0.65
21	0.67	0.63
22	0.7	0.6
23	0.38	0.51
24	0.58	0.52
25	0.4	0.47
26	0.5	0.54
27	0.44	0.46
28	0.29	0.55
29	0.41	0.5
30	0.46	0.48
31	0.41	0.57
32	0.31	0.41
33	0.49	0.7
34	0.39	0.29
35	0.28	0.35
36	0.31	0.38
37	0.4	0.35
38	0.46	0.42
39	0.36	0.42
40	0.32	0.35
41	0.27	0.4
42	0.4	0.47
43	0.34	0.45
44	0.33	0.33
45	0.42	0.42
46	0.4	0.5
47	0.35	0.32
48	0.32	0.44
49	0.32	0.48
50	0.35	0.3
51	0.33	0.67
52	0.33	0.5
53	0.32	0.38

Table 9: Results of maximum and minimum entropy.

N° BASIN	Informational Entropy
1	2.46
2	2.41
3	2.43
4	2.46
5	2.46
6	2.42
7	2.46
8	2.47
9	2.47
10	2.47
11	2.47
12	2.44
13	2.48
14	2.46
15	2.45
16	2.41
17	2.45
18	2.45
19	2.41
20	2.41
21	2.34
22	2.34
23	2.26
24	2.37
25	2.28
26	2.29
27	2.1
28	2.3
29	2.23
30	2.27
31	2.16
32	2.3
33	2.16
34	2.34
35	2.29
36	2.12
37	2.01
38	2.13
39	2.19
40	2.26
41	2.15
42	2.01
43	2.3
44	2.06
45	2.05
46	2.15
47	2.16
48	2.2
49	1.96
50	2
51	2.1
52	1.87
53	1.87

Table 10: Results of Informational Entropy**.**

6.Conclusions.

Mean daily streamflow data from several undisturbed independent watersheds in Switzerland were analyzed for changes with some statistical tools and some new stability index based on the concept of entropy.

The analysis was conducted on the original data series for the period 1971-2000.

The indexes used in this work never was used in literature to analyze the regime stability. Indexes are innovative and simple but effective tool of analysis, applicable to all data series in order to obtain a clear and simple vision of the regime stability. From the executed analysis, significant variations of regimes stability were not always pointed out.

The connection between streamflow and their associated watersheds has been investigated, in order to determine the nature of changes in streamflow.

The purpose of this correlation analysis is to examine if there is any attribute that could generate a change in hydrological regime.

For the period 1971-2000, streamflow results are well connected with basin attributes related to soil (mean soil depth, mean CN) and to land cover (glaciers and rock).

Even if the geomorphologic evolution within a watershed is much slower than possible changes in climate (due to anthropogenic influences), the analysis proved that certain hydrographical basin properties contribute to the vulnerability of the streamflow regime.

The streamflow results are in agreement with recent studies regarding precipitation trends in Switzerland conducted by Widmann & Schär (1997) and Frei & Schär (2001), where significant increases in winter precipitation were observed, and with previous studies in other hydrological variables, like temperature and snowmelt [Beniston *et al.*, 1994].

The geomorphologic evolution within a watershed is much slower than possible changes in climate, due to anthropogenic influences, and changes in the hydrologic regime especially in maximum flow are rather indicating a climatic change.

It is pointed out how the analysis was possible thanks to a wide and complete data set given by the Institute ETH of Zurich.

Considering the big amount of analyzed series, the data quality and spatial coverage, the big percentage of trends and their strong (summer) connections with large-scale climate anomalies, altogether, the results of this study are scientifically interesting.

References:

1. Arnell, N.W., 1998: Climate change and water resources in Britain. Climatic Change (39), 83–110.

2. Arnell, N.W., 2003: Relative effects of multi-decadal climatic variability and changes in the mean and variability of climate due to global warming future streamflows in Britain. Journal of Hydrology (270), 195-213.

3. Arnell, N.W., 1999a: The effect of climate change on hydrological regimes in Europe: a continental perspective. Global Environmental Change (9), 5–23.

4. Arnell, N.W., 1999b: Climate change and global water resources. Global Environmental Change (9), S31–S49.

5. Arnell, N.W., Krasovskaia, I., Gottschalk, L. 1993: River flow regimes in Europe. In: Flow Regimes from International Experimental and Network Data (FRIEND), ed. A. Gustard, Hydrological Studies (1), 112-121. Institute of Hydrology, Wallingford, UK.

6. Arnell, N.W. and N.S. Reynard, 1996: The effects of climate change due to global warming on river flows in Great Britain. Journal of Hydrology (183), 397–424.

7. Blöchliger, H., and Neidhöfer, F., Climate change in Switzerland. Effects of extreme precipitation events, Assessment Report, OcCC, 1999.

8. Brunetti, M., M. Maugeri, T. Nanni, 2000: Variations of temperature and precipitation in Italy from 1866 to 1995. Theoretical and Applied Climatology (65), 165–174.

9. Brunetti, M., Colacino, M., Maugeri, M., and T. Nanini, 2001: Trends in the daily intensity of precipitation in Italy. International Journal of Climatology (21), 299-316, 2001.

10. Bonsal BR, Zhang X, Hogg WD., 1999: Canadian Prairie growing season precipitation variability and associated atmospheric circulation. Climate Research (11), 191–208.

11. Burlando, P. Fraschini, E.M., Kuhne, A. Impact of climate change on river runoff in mountains areas. In: Ribamond. River Basin Management and Flood Mitigation. Concerned Action. pp. 251-268.

12. Burn, D. H., and Hag Elnur, M.A., 2002: Detection of hydrologic trends and variability. Journal of Hydrology (255), 107-122.

13. Frei, C., and C. Scha¨r, 1998: A precipitation climatology of the Alps from high-resolution rain-gauge observations. Int. J. Climatol. (18), 873–900.

14. Frei, C., and Schär, C., 2001: Detection probability of trends in rare events: theory and application to heavy precipitation in the alpine region, Journal of Climate (14), 1568-1584.

15. Gottschalk, L., Jensen, J.L., Lundquist, D., Solantie, R., Tollan, A., 1979: Hydrologic Regions in the Nordic Countries. Nordic Hydrology (10), 273-286.

16. Jones, P. D., et all, 1999: The use of indices to identify changes in climatic extremes. Climatic Change (42), 131-149.

17. Krasovskaia, I., 1997: Entropy-based grouping of river flow regimes. Journal of Hydrology (202), 173-191.

18. Krasovskaia, I., 1995: Quantification of the stability of river flow regimes. Hydrological Sciences Journal (40), 587–598.

19. Krasovskaia, I., Arnell, N.W., Gottschalk, L. 1994: Flow regimes in northern and Western Europe: development and application of procedures for classifying flow regimes. In: Flow Regimes from International Experimental and Network Data (FRIEND), ed. P. Seuna, A. Gustard, N. W. Arnell & G.A. Cole (Proc. 2nd Int. Conf., UNESCO, Braunschweig, Germany, October 1993), 185-193. IASH Publ. no.221.

20. Krasovskaia, I., Gottschalk, 1993: Frequency of Extremes and its Relation to Climate Fluctuation. Nordic Hydrology (24), 1-12.

21. Krasovskaia, I., Gottschalk, 1992: Stability of river flow regimes. Nordic Hydrology (23), 137-154.

22. Koppen, W., Das Geographisches System der Klimate, in Handbuch der Klimatologie (eds. Koppen, W., Geiger, R.),Berlin:Gebruder Borntraeger, 1936.

23. Intergovernmental Panel on Climate Change 1999 and 2001. (IPCC Report). Published by the press syndicate of the university of Cambridge.

24. Leith, R. M., Whitfield, P. H., 1998: Evidence of climate change effects on the hydrology of streams in south-central B.C.. Can. Water Resour. J. (23), 219-231.

25. Lvovich, M., 1973: The World's Water. Mir, Moscow, pp. 205-245.

26. Middelkoop, H., et all, 2001: Impact of climate change on hydrological regimes and water resources management in the Rhine Basin. Climatic Change (49), 105-128.

27. Molnár, P., and Ramirez, J., 2001: Recent trends in precipitation and streamflow in the Rio Puerco Basin. Journal of Climate (14), 2317-2328.

28. Pfaundler, M., 2001: Adapting, analyzing and evaluating a flexible Index Flood regionalisation approach for heterogeneous geographical environments. PhD Dissertation, IHW 008, ETH Zürich, 189 pp.

29. Rebetez, M., M., Beniston, 1998: Changes in sunshine duration are correlated with changes in daily temperature range this century: an analysis of Swiss climatological data. Geophysical Research Letters (25), 3611–3613.

30. Salas, J. D., J. W. Delleur, V. Yevjevich, and W. L. Lane, Applied modeling of hydrologic time series, Water Resour. Publ., Littleton, Colo., 1980.

31. Widmann, M., and Schär, C., 1997: A principal component and long-term trend analysis of daily precipitation in Switzerland. International Journal of Climatology (17), 1333-135

Appendix 1
Switzerland Map

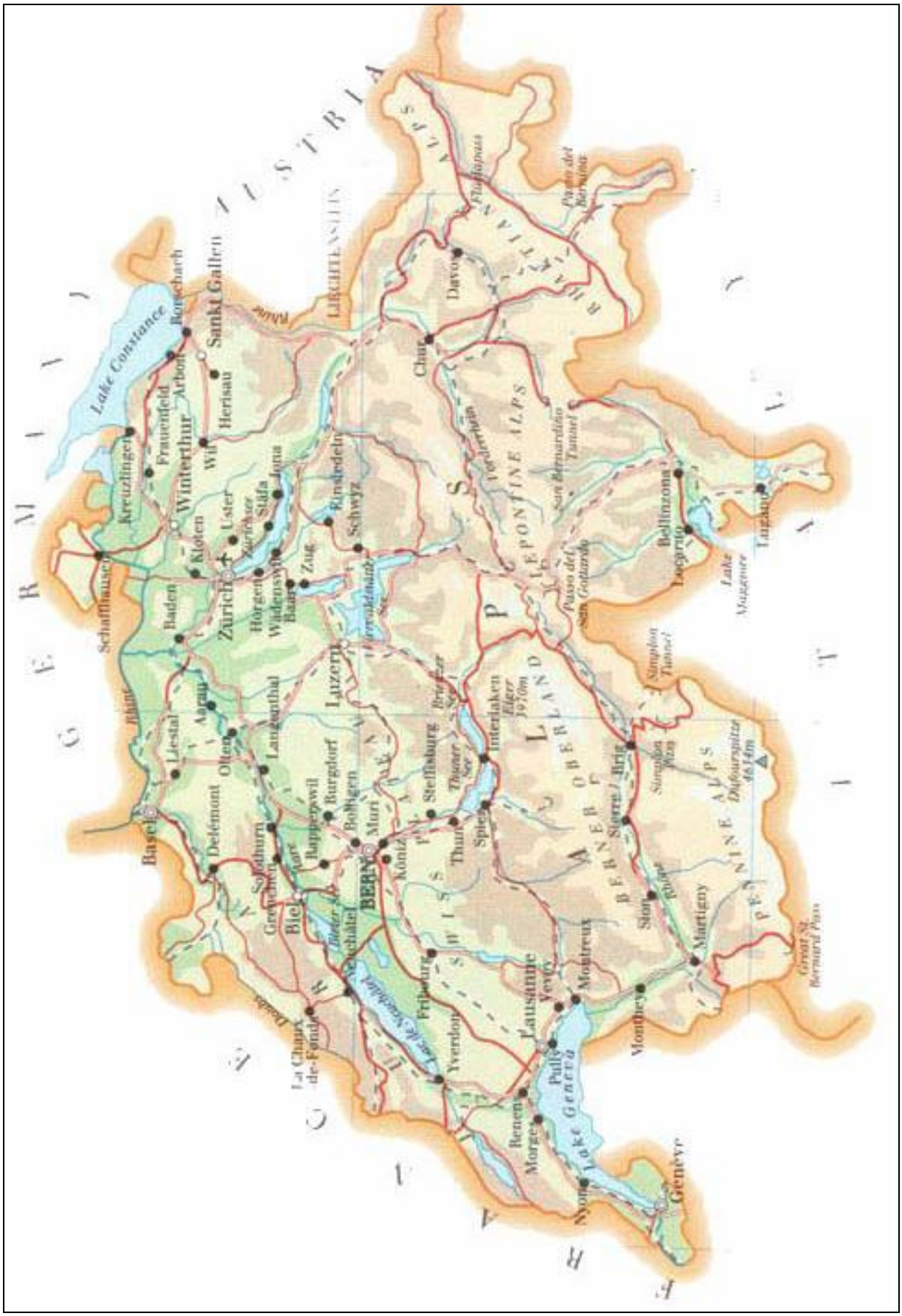

Appendix 2

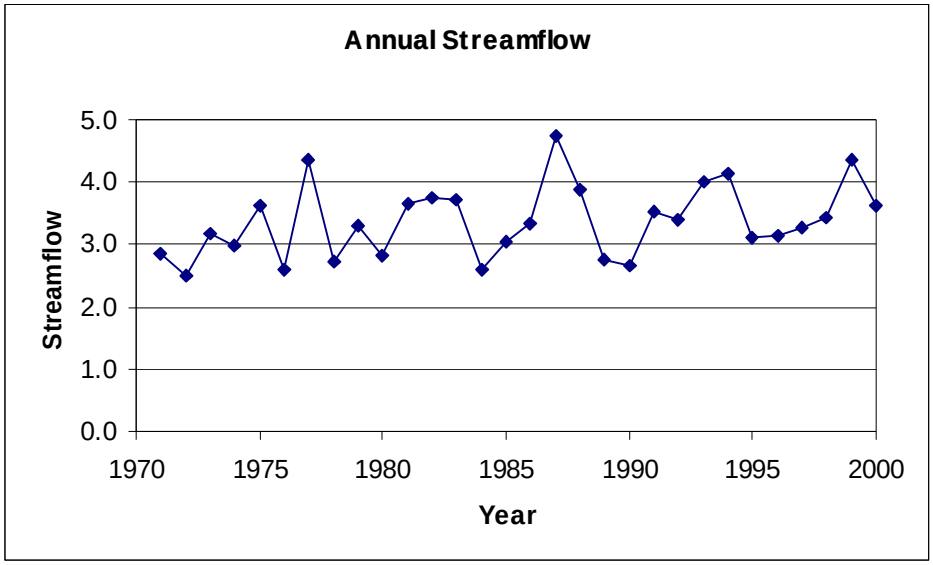

Fig 1 Annual streamflow time series

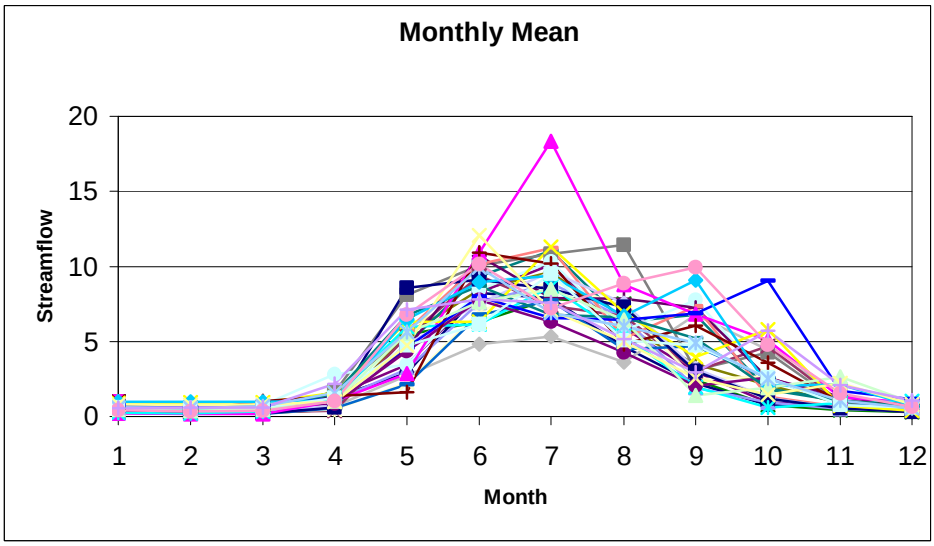

Fig 2: Monthly streamflow time series

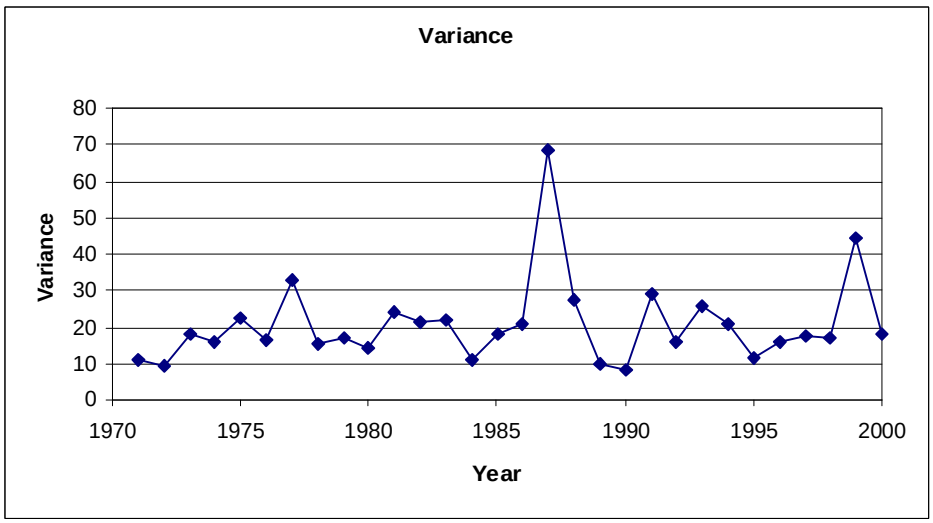

Fig.3 Time series of annual streamflow variance of daily data

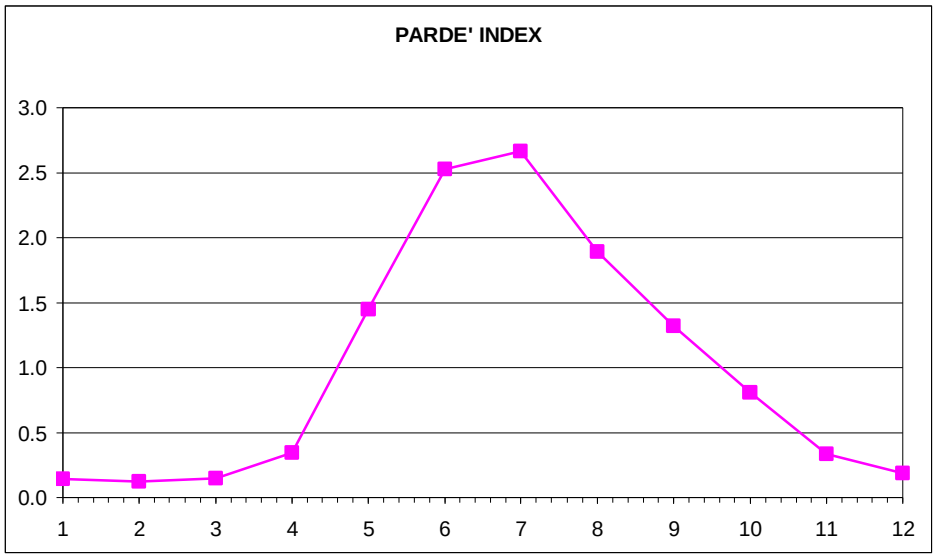

Fig. 4 Pardè Coefficient

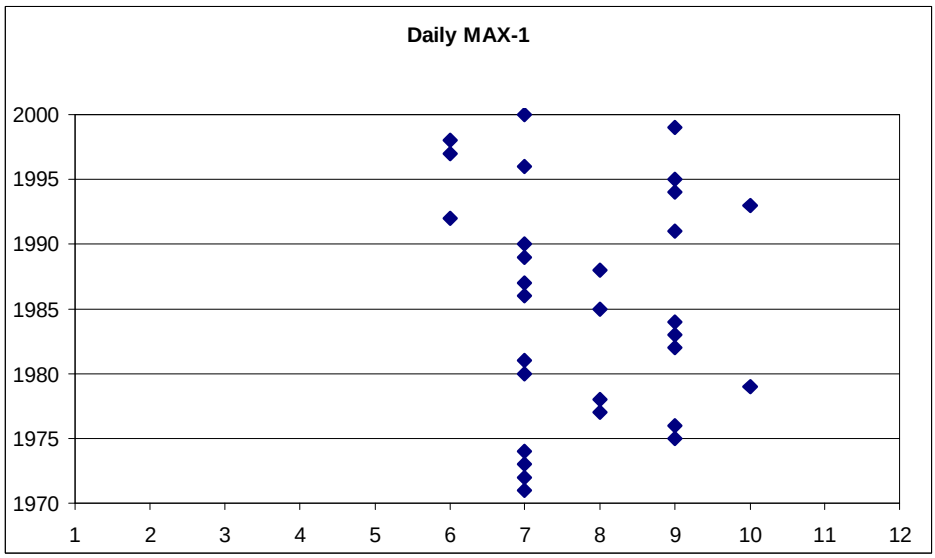

Fig.5 Time series of the Julian day in which the first maximum daily streamflow occur

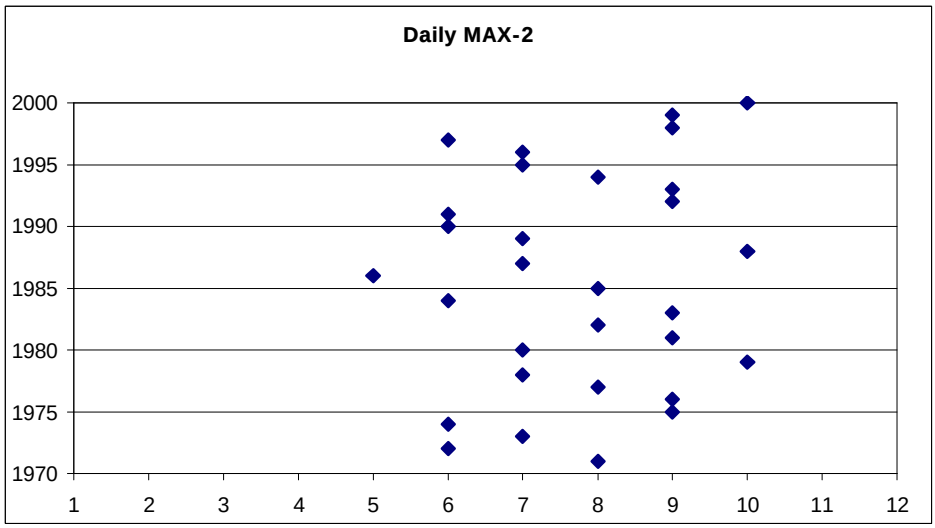

Fig.6 Time series of the Julian day in which the second maximum daily streamflow occur

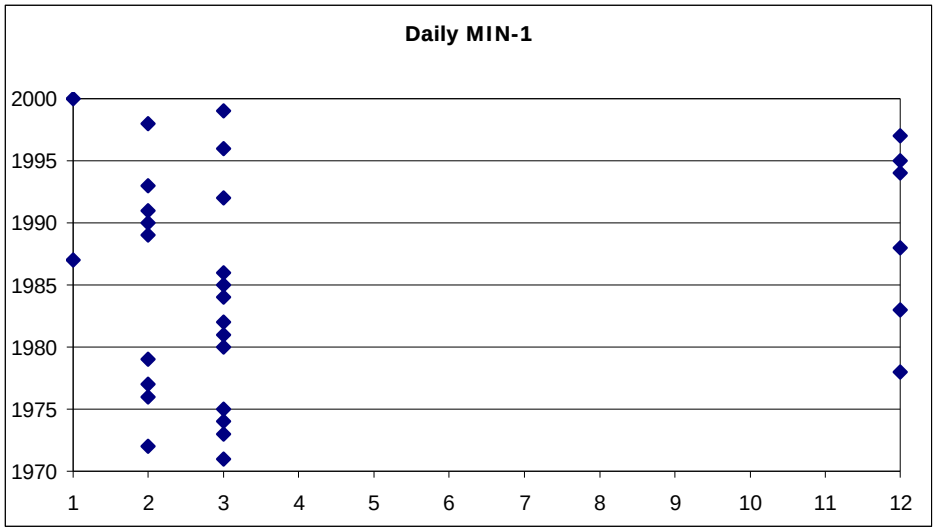

Fig.7 Time series of the Julian day in which the first minimu daily streamflow occur

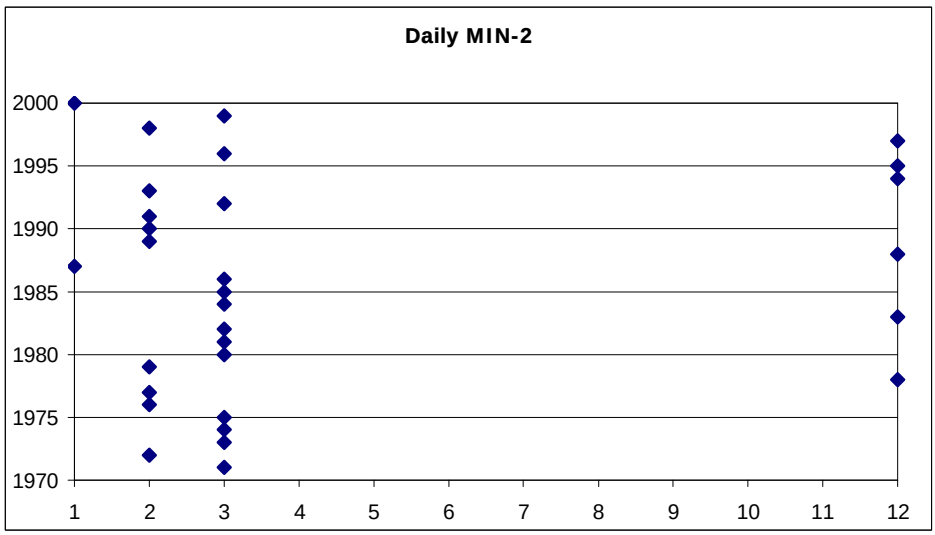

Fig.8 Time series of the Julian day in which the second minimu daily streamflow occur

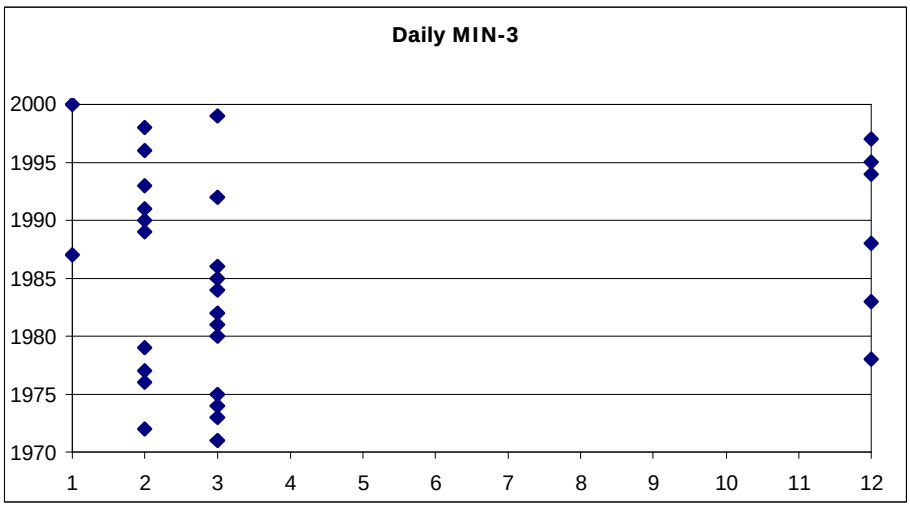

Fig.9 Time series of the Julian day in which the third minimu daily streamflow occur

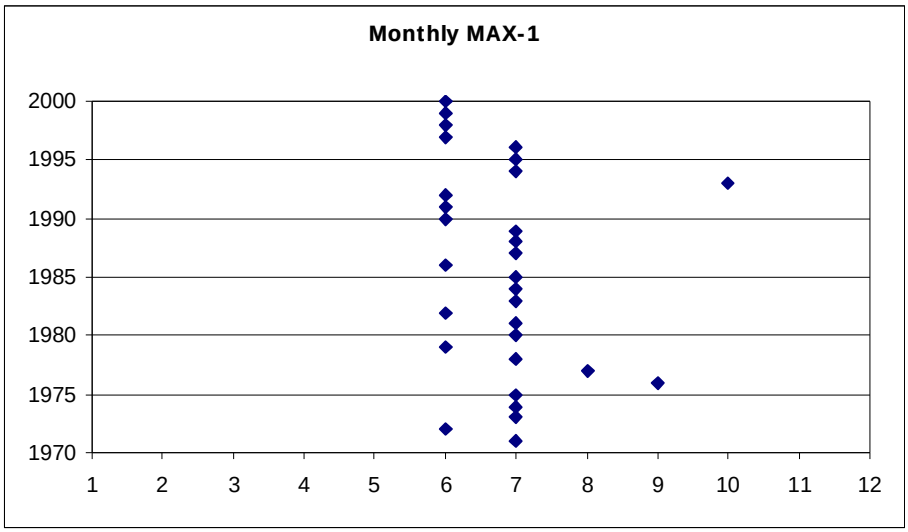

Fig. 10 Time series of the first maximum month of the year in which streamflow occur

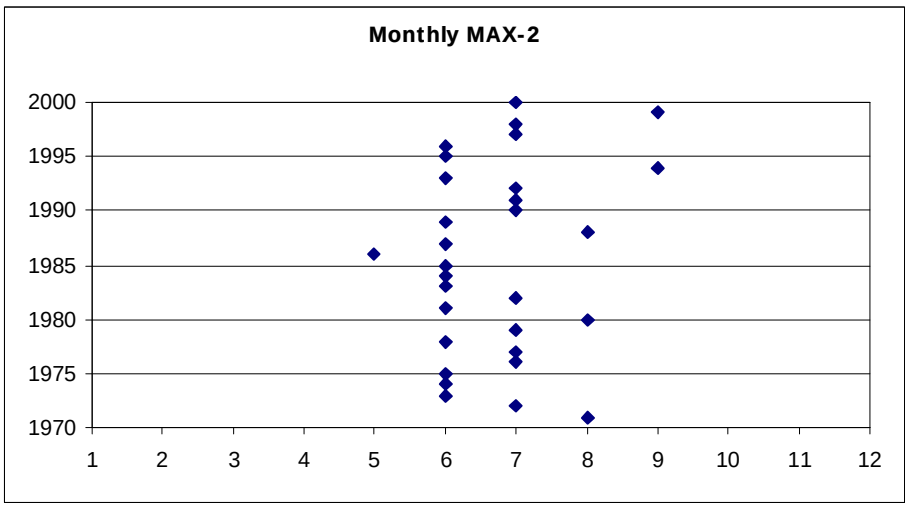

Fig. 11 Time series of the second maximum month of the year in which streamflow occur

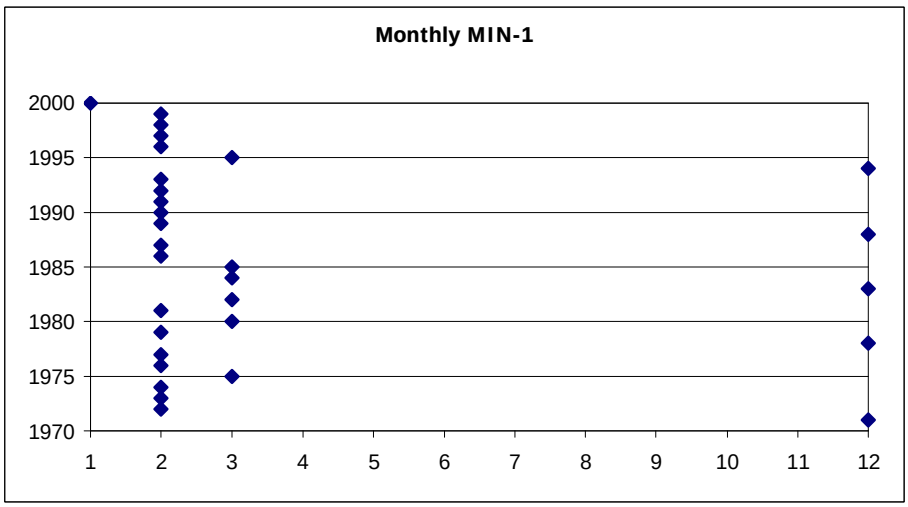

Fig. 12 Time series of the first minimum month of the year in which streamflow occur

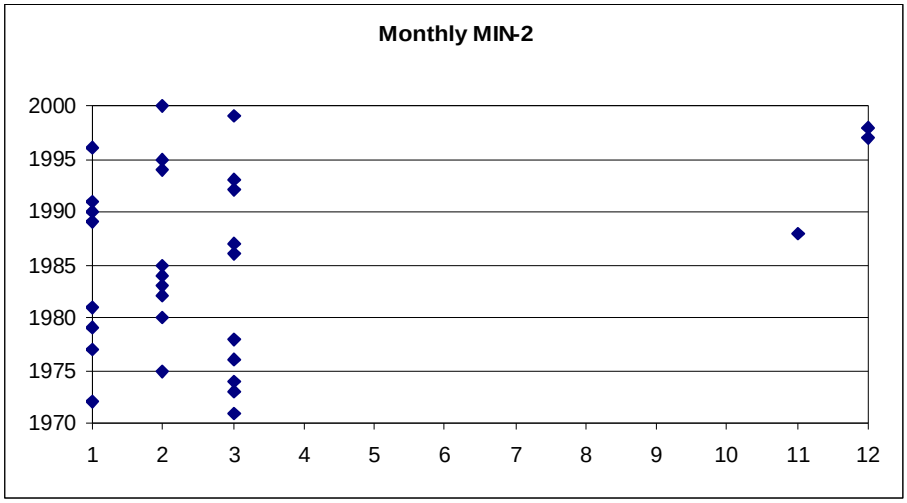

Fig. 13 Time series of the second minimum month of the year in which streamflow occur

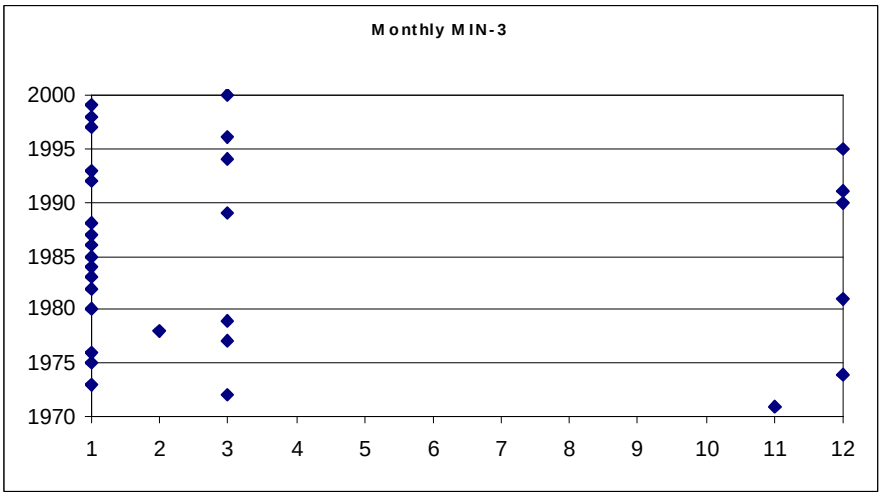

Fig. 14 Time series of the third minimum month of the year in which streamflow occur

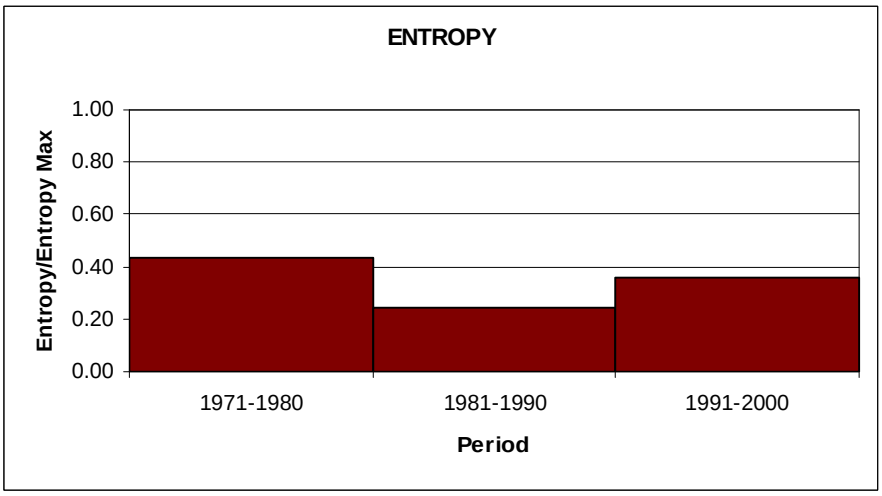

Fig. 15 Time series of the Informational Entropy related to maximum monthly streamflow

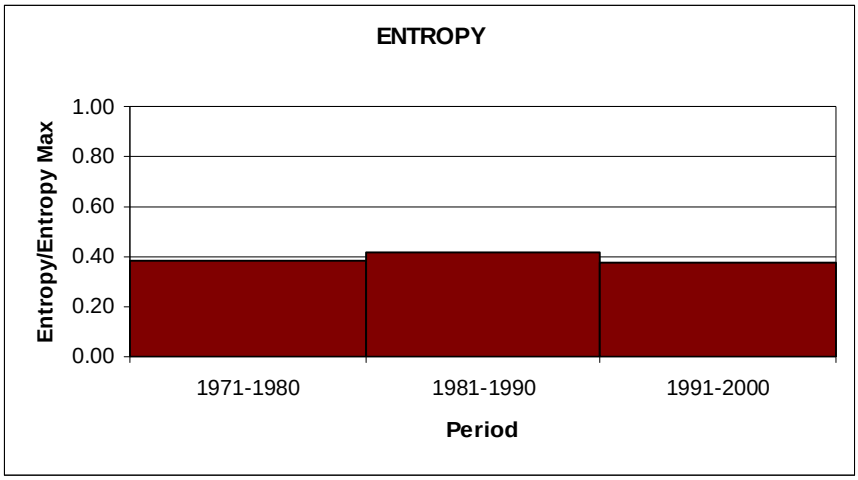

Fig. 16 Time series of the Informational Entropy related to minimum monthly streamflow

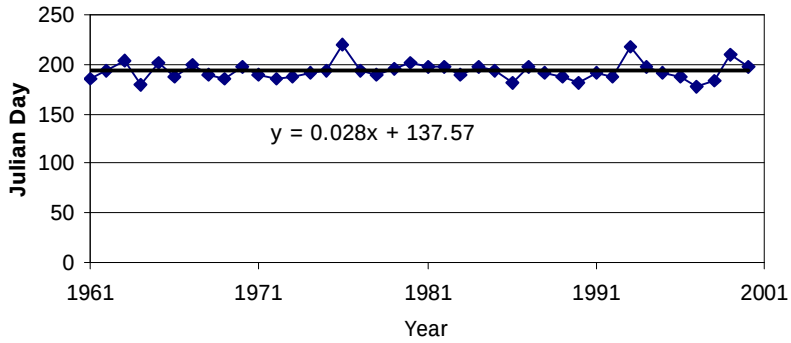

Fig. 17 Time span underlying half of the runoff volume in each year

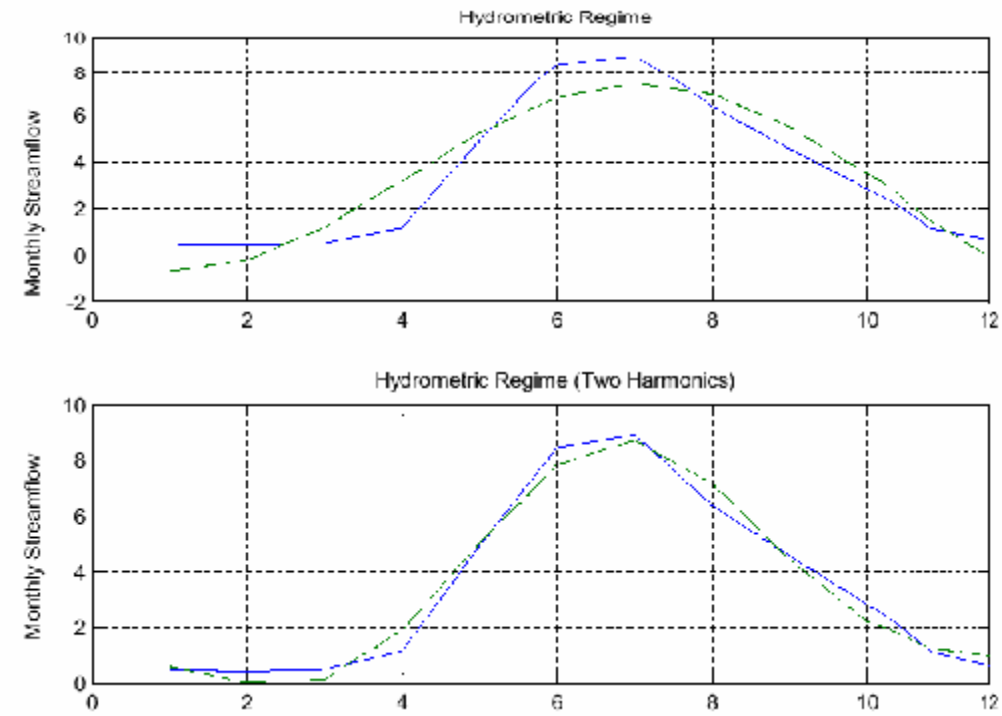

Fig. 18 Time series of the streamflow average regime interpolated by the Fourier series

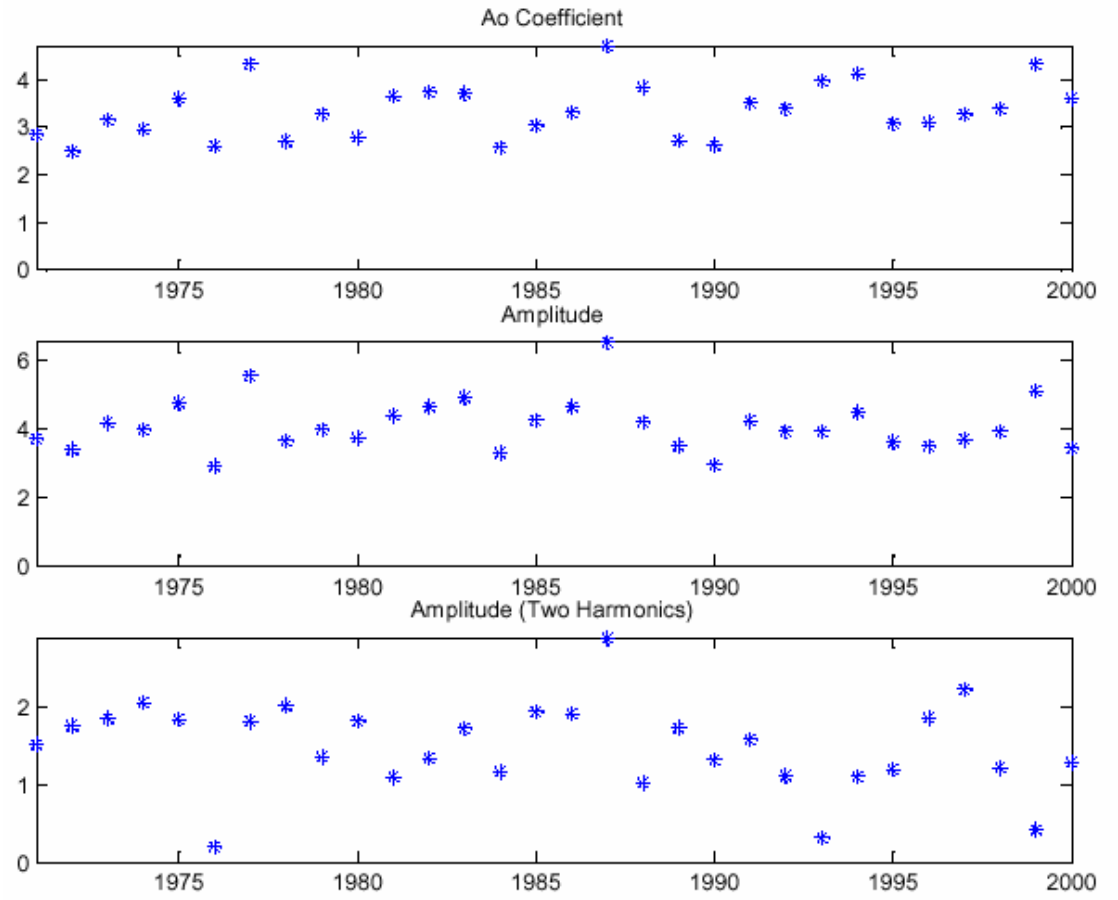

Fig 19 Time series of the annual estimate of the Fourier series amplitude

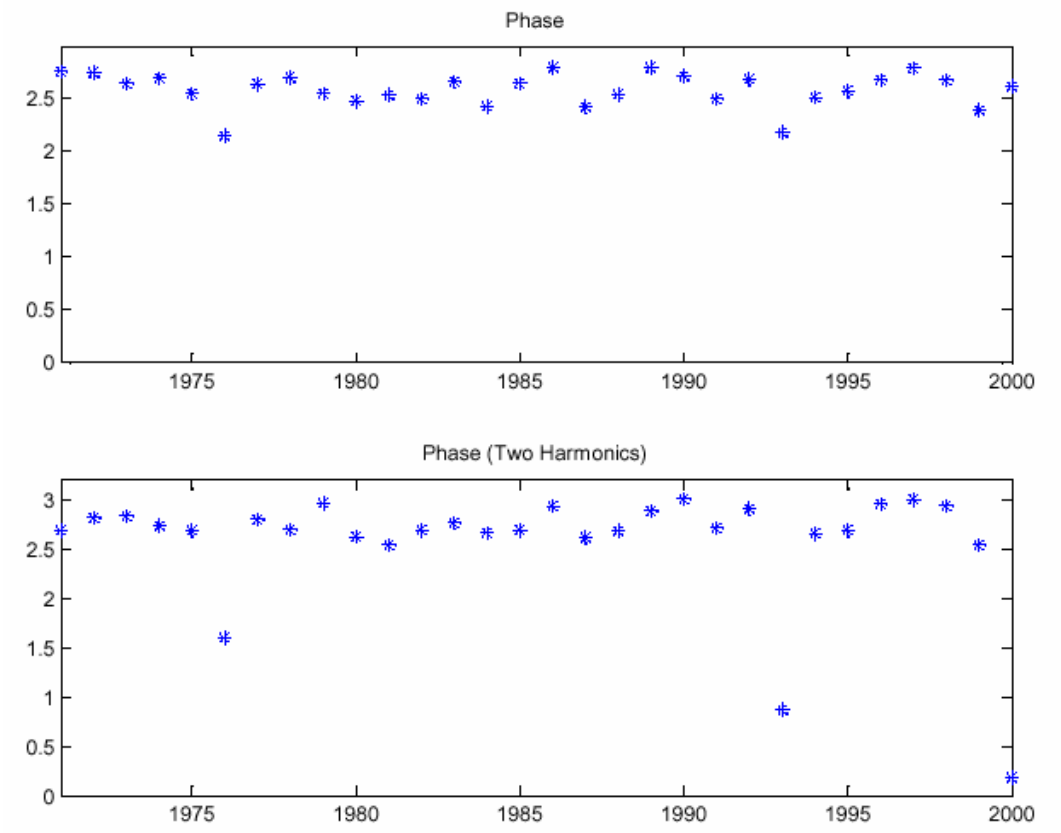

Fig 20 Time series of the annual estimate of the Fourier series phase